Nanomanufacturing

University of Michigan

ME599-002 | Winter 2010

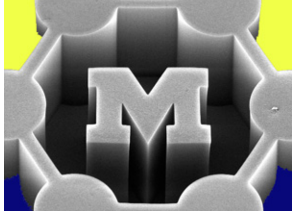

18: Self-assembly of micelles and block copolymers

March 29, 2010

John Hart

ajohnh@umich.edu

http://www.umich.edu/~ajohnh

Announcements

- Project proposals will be available tomorrow (Tuesday)
- Peer reviews due Friday
- Please identify your teams and decide your project topic ASAP
- Sign up for a 15 minute meeting with John
    - Thursday 4-6 PM or Sunday 1-3 PM, 2278 GGB
    - http://bit.ly/cBNAxk
    - Meeting will focus on
        - Definition of key idea
        - Proposed details/feasibility of the idea
        - Expected analysis based on course material
        - Anything else..
    - If possible your entire team should attend
    - Off-campus by phone
- No normal office hours this week (project meetings instead)

Recap: post-processing

- **Purification**
  - Remove impurities such as undesired byproducts, unreacted catalyst
  - Anneal to improve crystallinity
  - Etch to control size

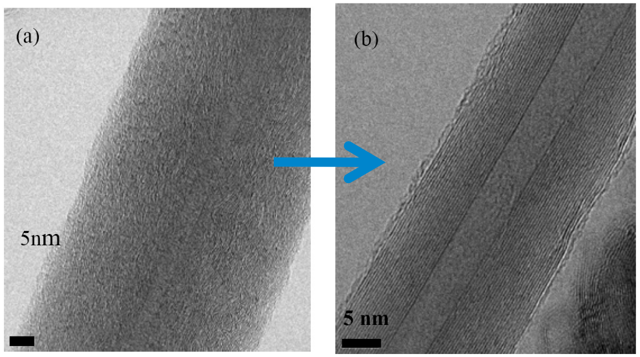

- **Stabilization and functionalization**
  - Attach/associate molecules with nanomaterial surfaces to facilitate interaction with other materials and phases

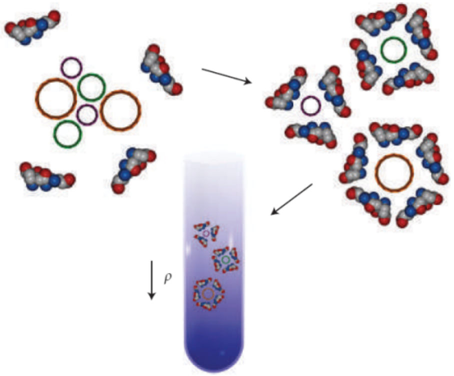

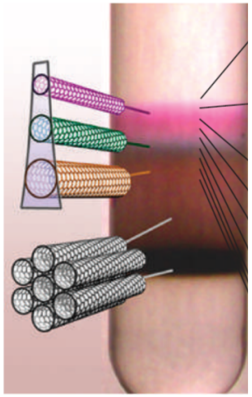

- **Separation/sorting**
  - Partition elements by size, shape, and/or electronic structure

A combination of methods usually seeks the desired final result (e.g., seed amplification)

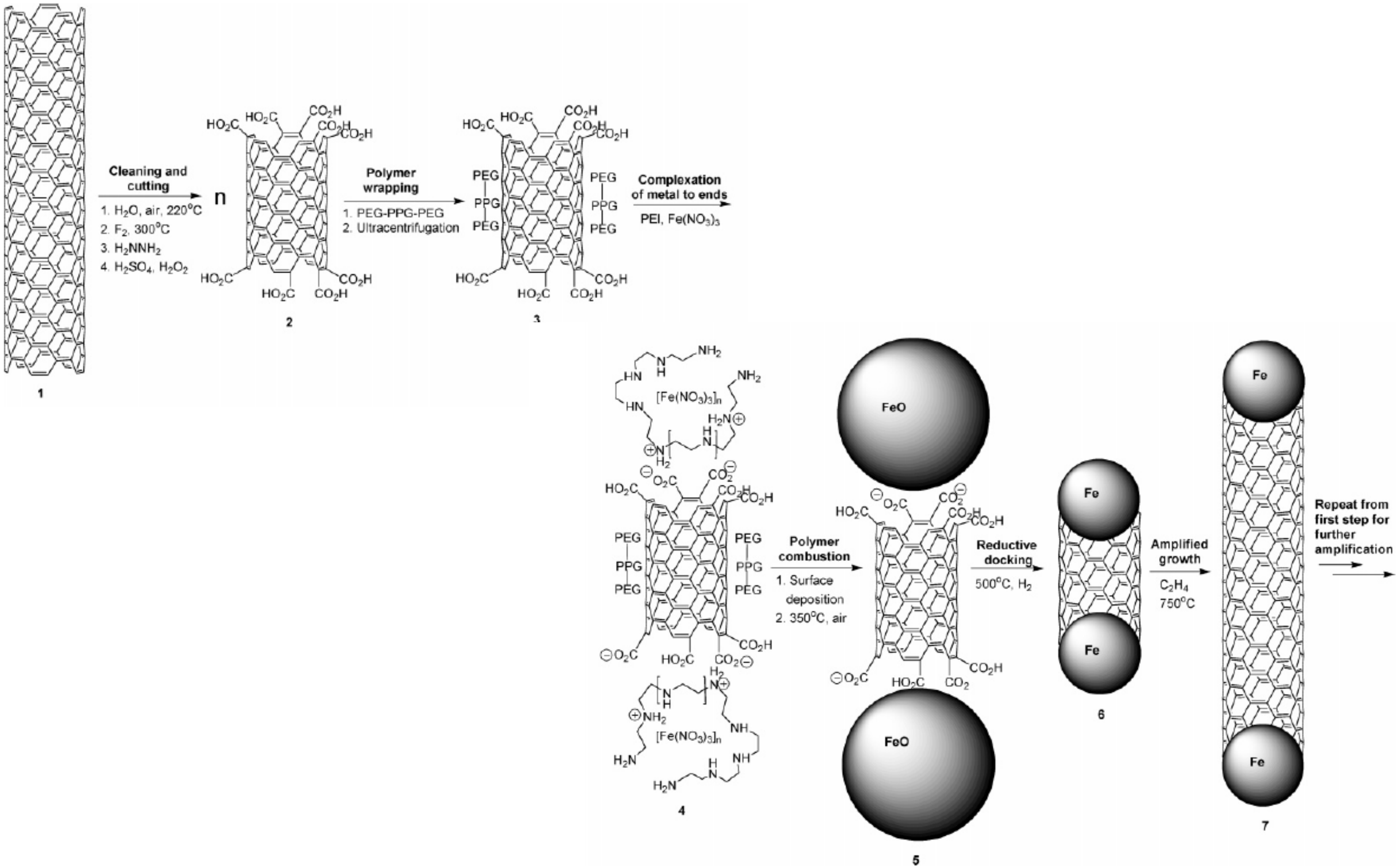
Scheme 1. A Depiction of the Amplification Growth Process of a Carbon Nanotube

Smalley, Tour, et al.

Restarting CNT growth

- Chirality does not match

Original +Fe at end

Restart

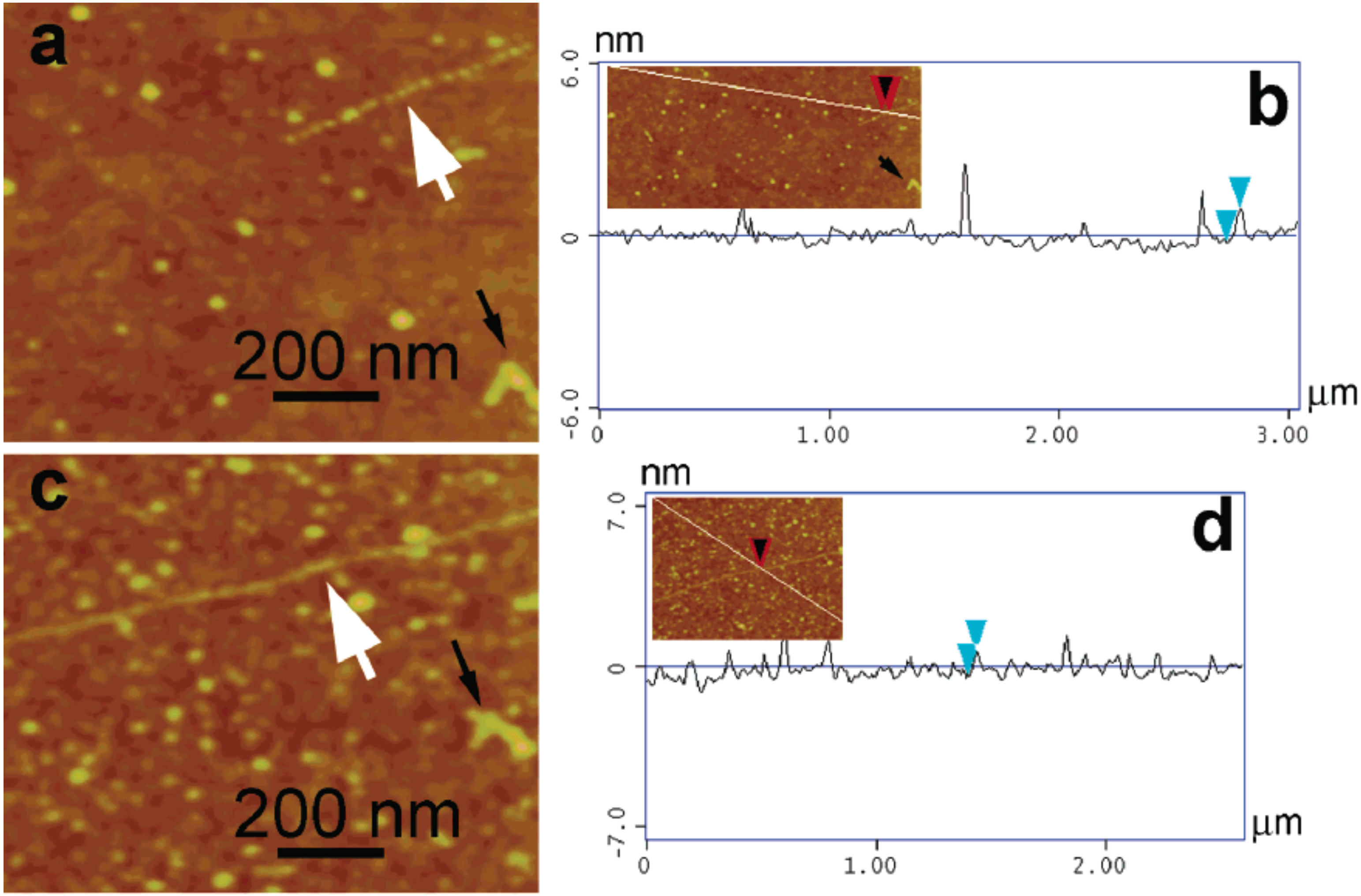

Smalley, Tour, et al.

From synthesis to assembly

0D

- Cluster synthesis (chemical/physical)
- Nanoparticle synthesis (chemical/physical)
- “Short” molecule synthesis (chemical)

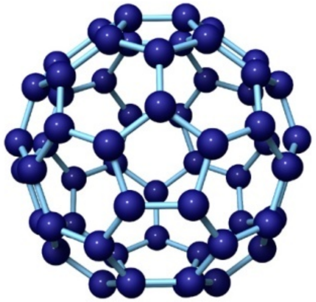

1D

- Nanotube/nanowire synthesis (chemical/physical)
- Nanoparticle assembly into chains (chemical)
- “Long” molecule synthesis (chemical/mechanical)

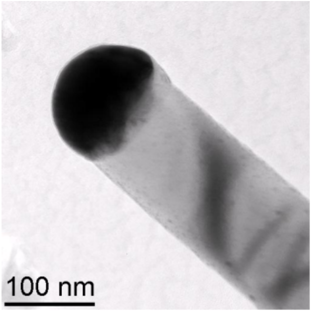

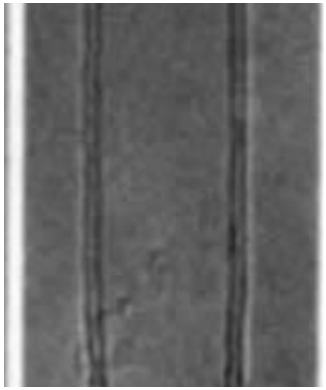

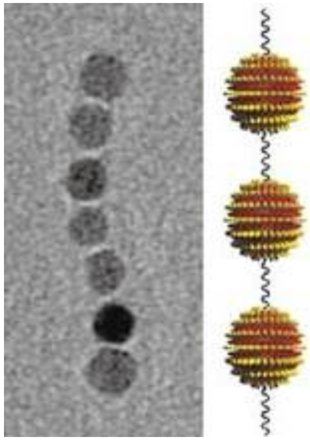

From synthesis to assembly

2D

- Film deposition and growth (physical/chemical):
  - growth of films of nanotubes/wires
  - monolayer self-assembly

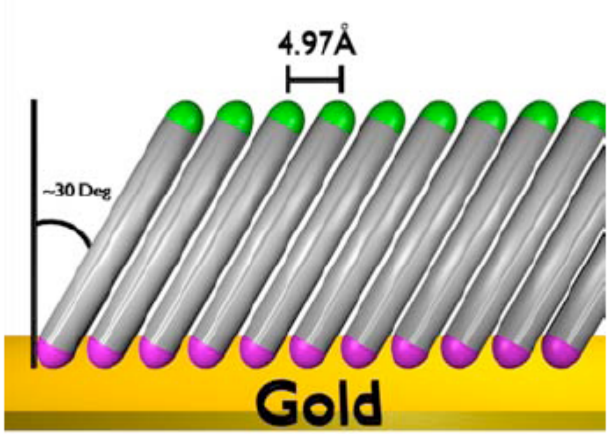

3D (all effects together)

- Colloidal crystals, superlattices
- Yarn spinning, networks, aerogels, composites, etc.

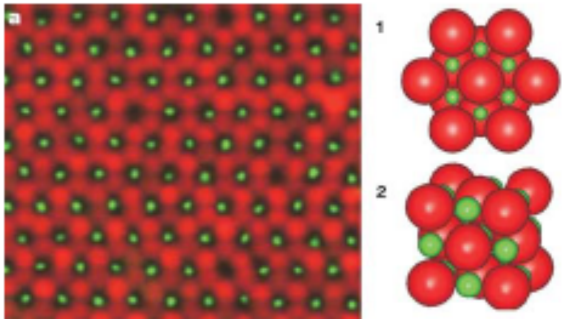

The goal is to maintain order as we scale up!

Limits of "top down" patterning

~10-100 nm resolution limits; mainly 2D

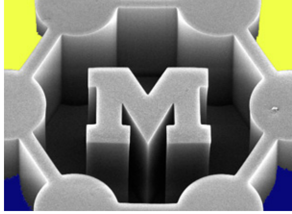

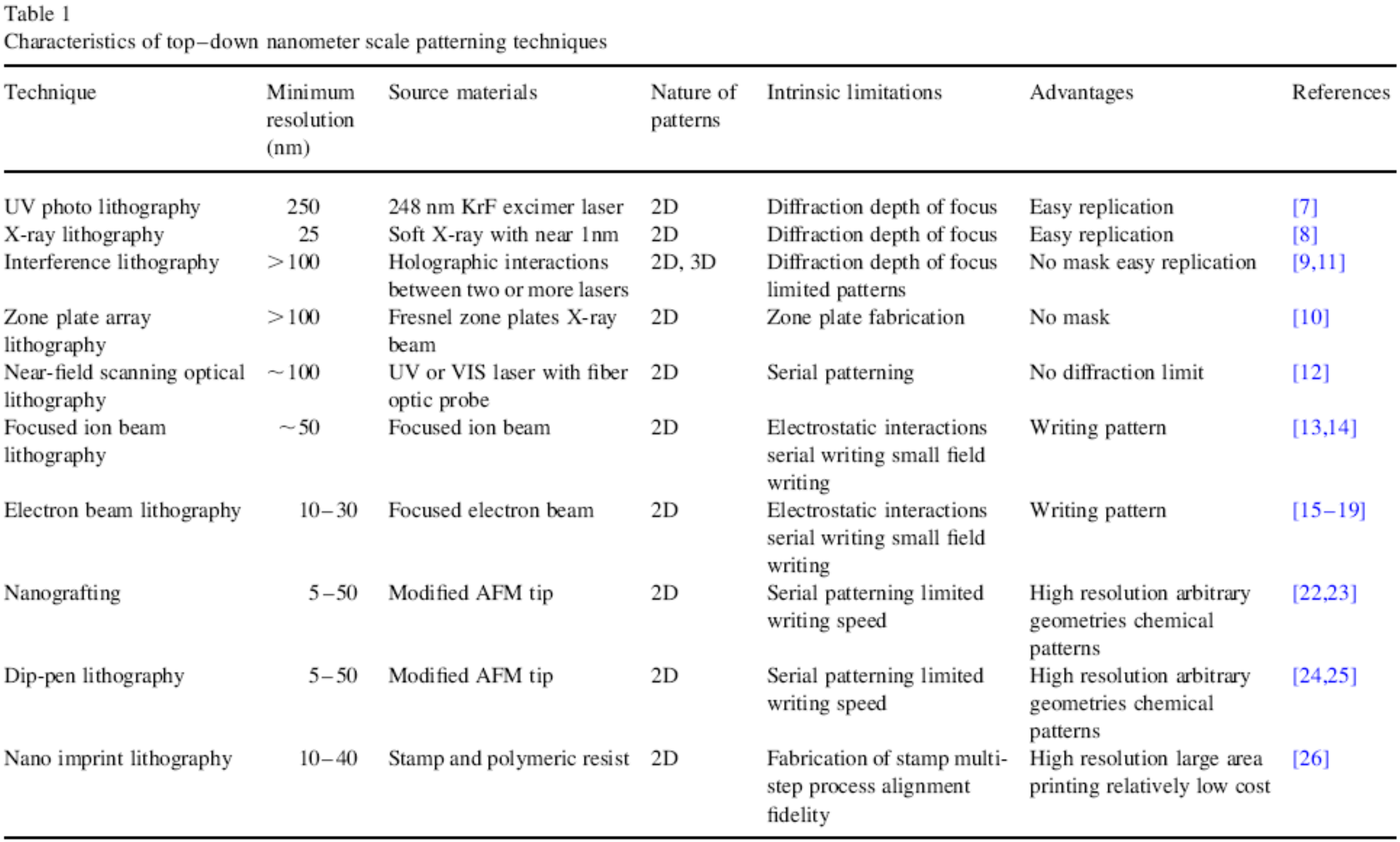

Table 1

Characteristics of top–down nanometer scale patterning techniques

Technique	Minimum resolution (nm)	Source materials	Nature of patterns	Intrinsic limitations	Advantages	References
UV photo lithography	250	248 nm KrF excimer laser	2D	Diffraction depth of focus	Easy replication	[7]
X-ray lithography	25	Soft X-ray with near 1nm	2D	Diffraction depth of focus	Easy replication	[8]
Interference lithography	>100	Holographic interactions between two or more lasers	2D, 3D	Diffraction depth of focus limited patterns	No mask easy replication	[9,11]
Zone plate array lithography	>100	Fresnel zone plates X-ray beam	2D	Zone plate fabrication	No mask	[10]
Near-field scanning optical lithography	~100	UV or VIS laser with fiber optic probe	2D	Serial patterning	No diffraction limit	[12]
Focused ion beam lithography	~50	Focused ion beam	2D	Electrostatic interactions serial writing small field writing	Writing pattern	[13,14]
Electron beam lithography	10–30	Focused electron beam	2D	Electrostatic interactions serial writing small field writing	Writing pattern	[15–19]
Nanografting	5–50	Modified AFM tip	2D	Serial patterning limited writing speed	High resolution arbitrary geometries chemical patterns	[22,23]
Dip-pen lithography	5–50	Modified AFM tip	2D	Serial patterning limited writing speed	High resolution arbitrary geometries chemical patterns	[24,25]
Nano imprint lithography	10–40	Stamp and polymeric resist	2D	Fabrication of stamp multi-step process alignment fidelity	High resolution large area printing relatively low cost	[26]

Park et al. *Polymer* 44:6725-6760, 2003.

Self-assembly

Interactions **balance** to give an equilibrium separation

Self-assembly
Motion and reversibility
= error-correction
= **order**

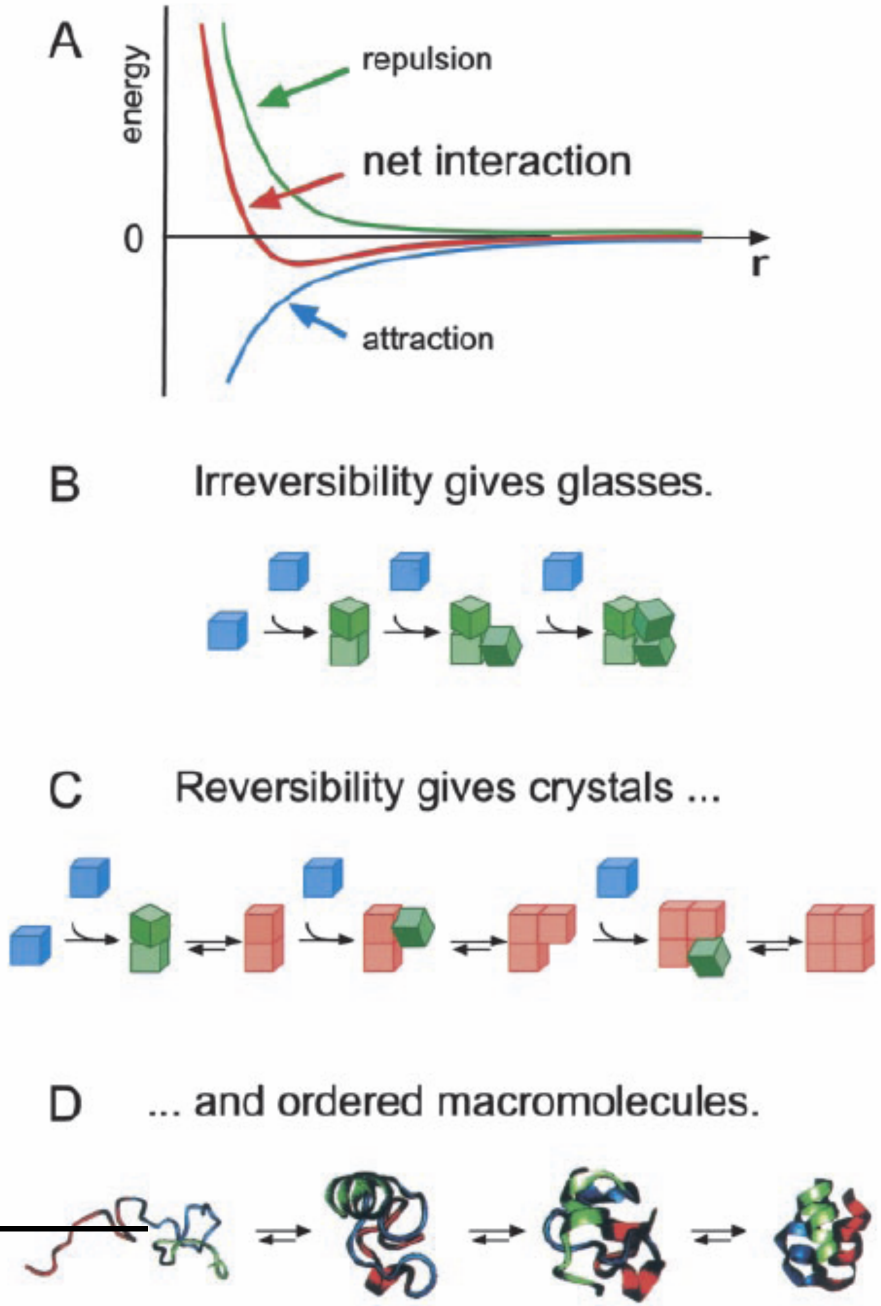

Fig. 1. (*A*) Aggregation occurs when there is a net attraction and an equilibrium separation between the components. The equilibrium separation normally represents a balance between attraction and repulsion. These two interactions are fixed in molecular self-assembly but can be engineered independently in macroscopic self-assembly. (*B* and *C*) Schematic illustration of the essential differences between irreversible aggregation and ordered self-assembly. (*B*) Components (shown in blue) that interact with one another irreversibly form disordered glasses (shown in green). (*C*) Components that can equilibrate, or adjust their positions once in contact, can form ordered crystals if the ordered form is the lowest-energy form (shown in red). (*D*) Biology provides many examples of self-assembly (here, the formation of a protein, an asymmetric, catalytically active nanostructure); these examples will stimulate the design of biomimetic processes.

Whitesides and Boncheva, *PNAS* 99(8):4769, 2002.

More ways to create anisotropy

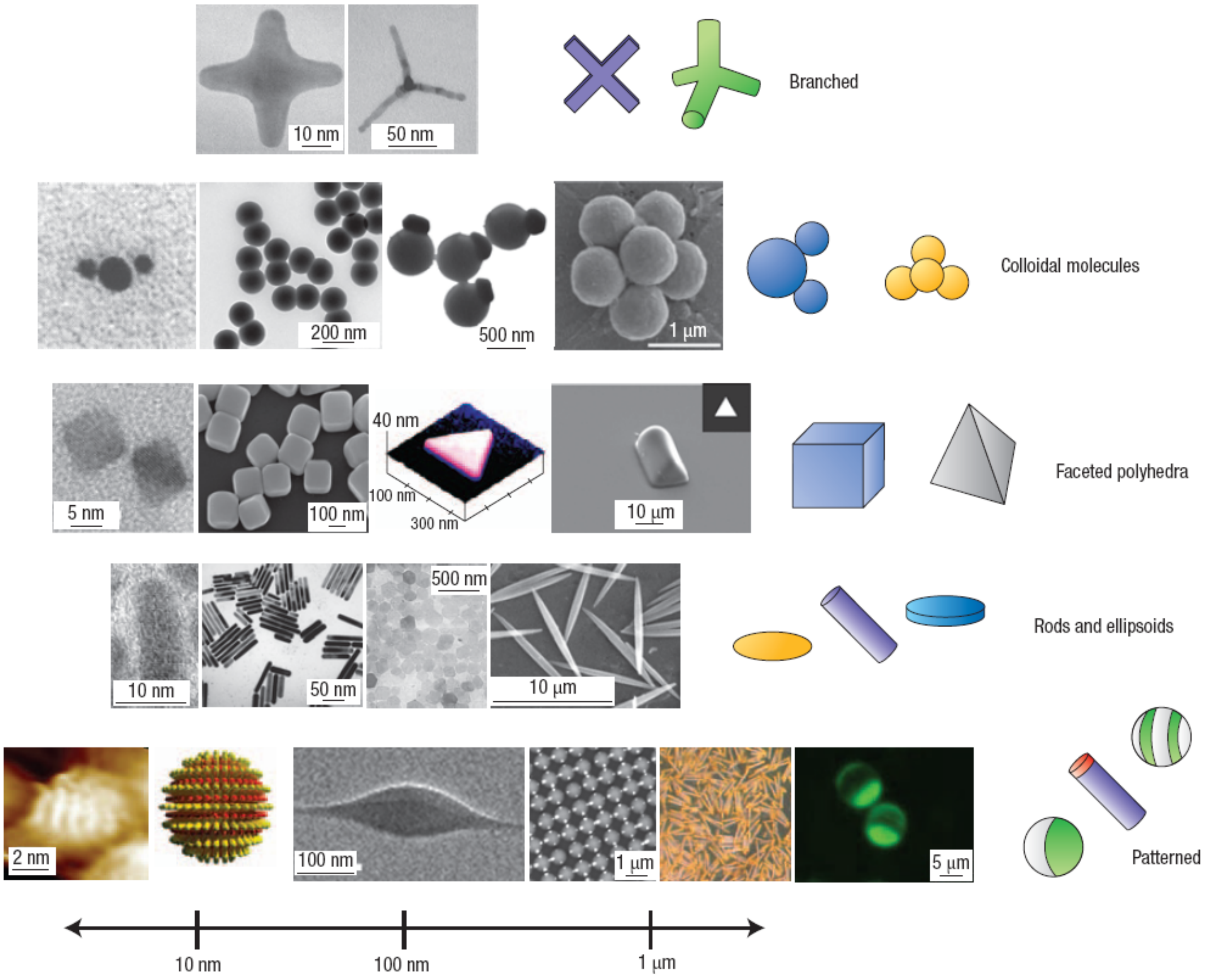

Glotzer and Solomon. *Nature Materials* 6:557-562, 2007.

Today's agenda

- Self-assembly of aggregates in solution
- Micelle techniques for nanoparticle synthesis
- Block copolymers

Today’s readings

Nominal: (ctools)

- Israelachvili, “Thermodynamic principles of self-assembly”
- Bates and Fredrickson, “Block copolymers – designer soft materials”

Extras: (ctools)

- Li et al., “Alternating patterns on single walled carbon nanotubes”
- Park et al., “Enabling nanotechnology with self assembled block copolymer patterns”

Amphiphile

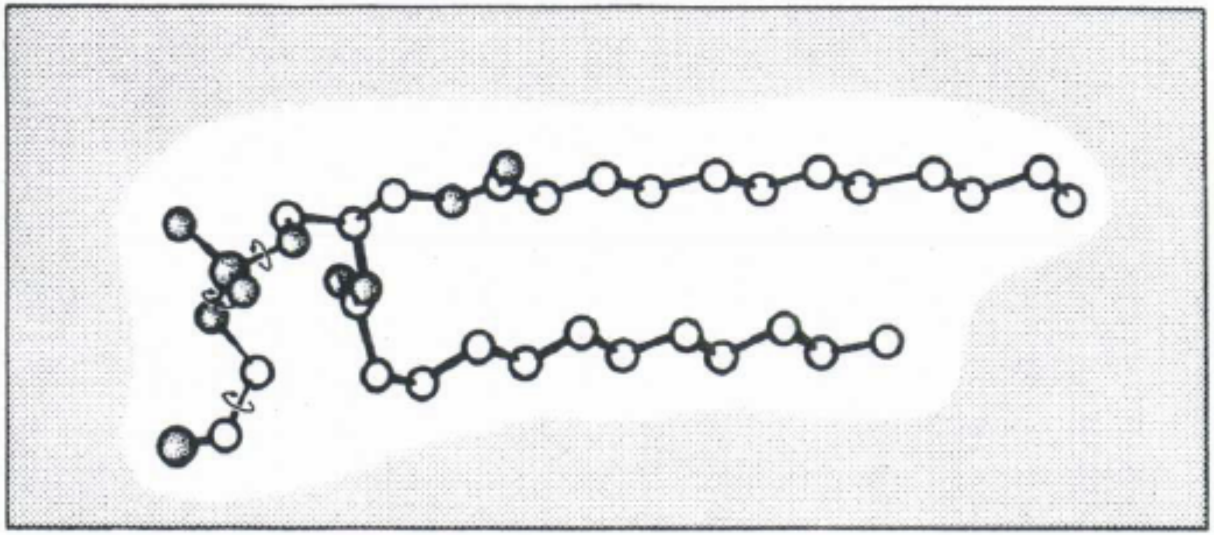

Fig. 16.2. The zwitterionic phospholipid dilauryl-phosphatidyl-ethanolamine containing two saturated hydrocarbon chains and a polar (hydrophilic) headgroup (see also Table 16.1).

Israelachvili.

Structures made from amphiphiles

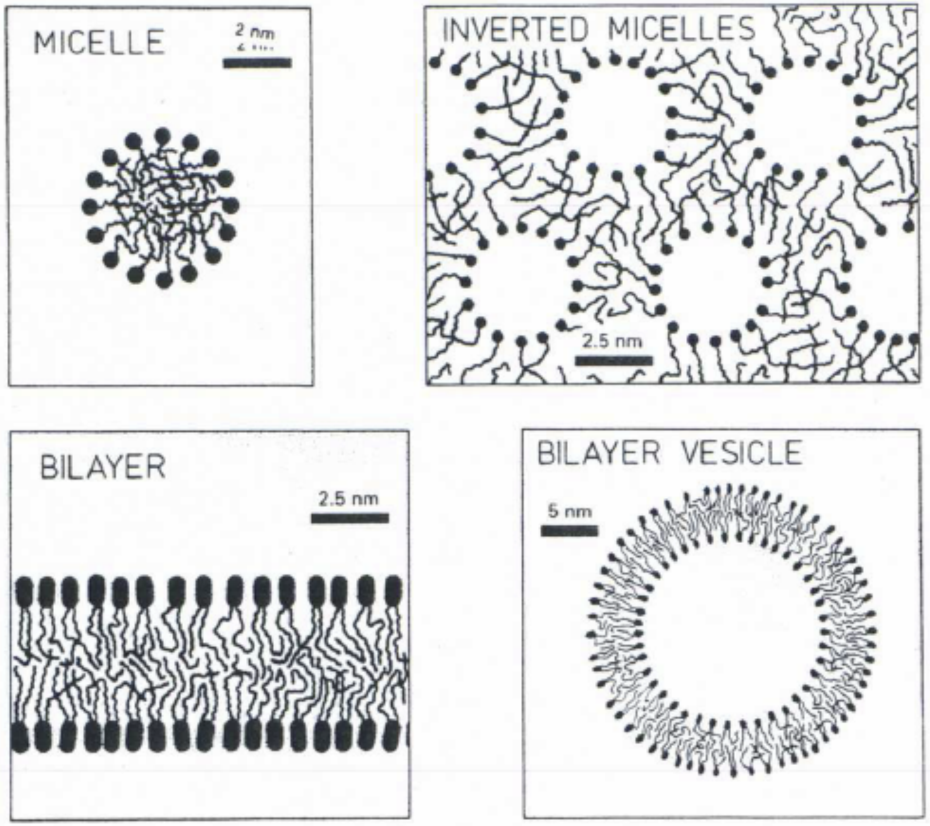

Fig. 16.1. Amphiphiles such as surfactants and lipids (see Table 16.1) can associate into a variety of structures in aqueous solutions. These can transform from one to another by changing the solution conditions such as the electrolyte or lipid concentration, pH, or temperature. In most cases the hydrocarbon chains are in the fluid state allowing for the passage of water and ions through the narrow hydrophobic regions, e.g., across bilayers. The lifetime of water molecules in lecithin vesicles is about 0.02 s, while ions can be trapped for much longer times, about 8 h for Cl^- and one month for Na^+ ions. Most single-chained surfactants form micelles, while most double-chained surfactants form bilayers, for reasons that are discussed in Chapter 17.

- Spontaneous self-assembly due to non-bonding interactions
- Continuous association and dissociation
- Size distributions
- Can change size/shape with changing solution conditions (e.g., concentration, pH)

Israelachvili.

Formation of aggregates

- X_N = dimensionless molar fraction of monomers that are in the N^{th} aggregation state

hydrophobic

hydrophilic

$$c_N = \frac{X_N}{N}$$

↑ concentration of aggregate

X_N

↑ concentration of monomer in Nth aggregate

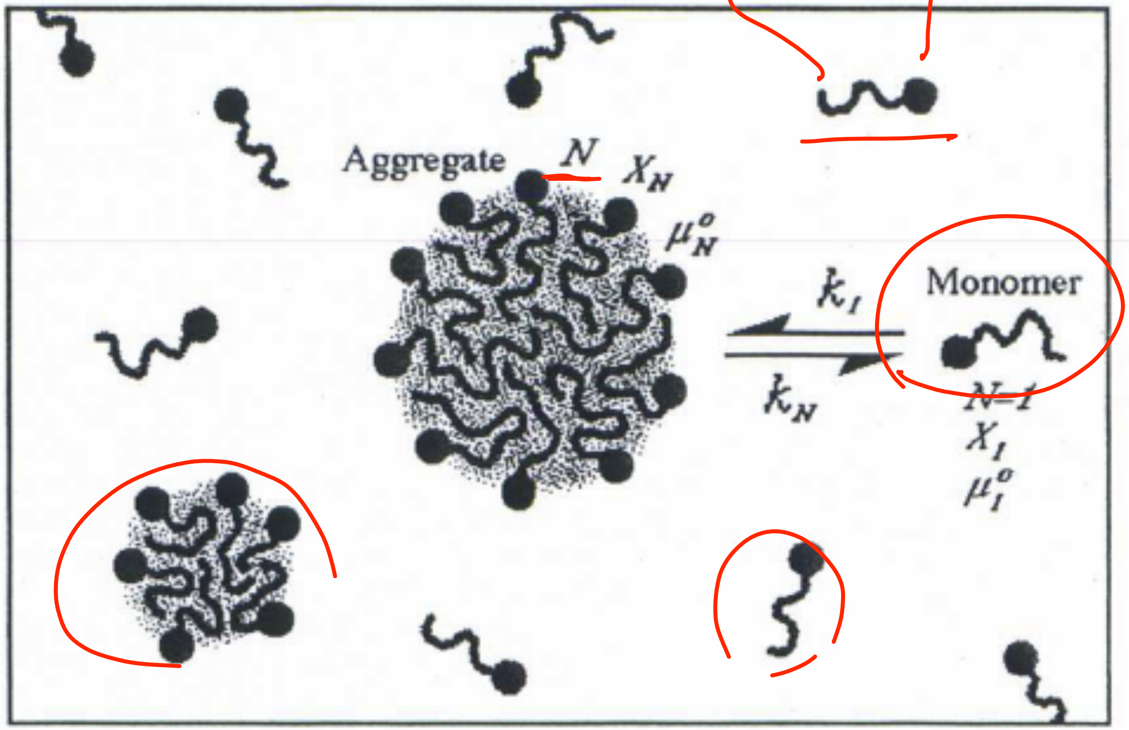

Fig. 16.3. Association of N monomers into an aggregate (e.g., a micelle). The mean lifetime of an amphiphilic molecule in a small micelle is very short, typically 10^{-5}–10^{-3} s.

total concentration

$$C = X_1 + X_2 + X_3 \cdots X_N = \sum_{N=1}^{\infty} X_N$$

Israelachvili.

Modeling aggregation kinetics

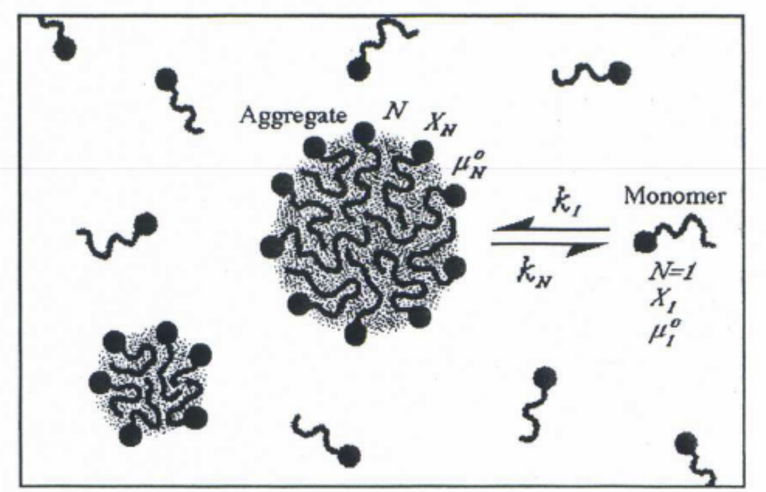

Mean interaction energy per molecule in the aggregate

c.p.

$$\underbrace{\tilde{\mu}} = \underline{\mu_N^\circ} + \frac{k_b T}{N}\ln\left(\frac{X_N}{N}\right) = \text{constant}$$

Mean chem potential of a monomer in any state n

1, 2, N

"reaction"

$$N X_1 \rightarrow \left(\frac{X_N}{N}\right)$$

N monomers

1 aggregate of size N

association

equilibrium constant, $K = \frac{k_a}{k_d}$

dissociation

$$= \exp\left(\frac{\Delta G}{k_b T}\right) = \exp\left(\frac{-N(\mu_N^\circ - \mu_1^\circ)}{k_b T}\right)$$

rate of $\underline{\text{association}}$: $\underline{k_a X_1^N}$

||

rate of $\underline{\text{dissociation}}$: $\underline{k_d \frac{X_N}{N}}$

$$\underline{n}\,\underline{A} + \underline{m}\,\underline{B} \longrightarrow C + D$$

$$\frac{d[C]}{dt} = k(T)[A]^n[B]^m$$

↑

eq. const

equilibrium

$$k_a X_1^N = k_d \frac{X_N}{N}$$

$$K = \frac{k_a}{k_d} = \left(\frac{X_N}{N}\right)\left(\frac{1}{X_1^N}\right) = \exp\left(\frac{-N(\mu_N^0 - \mu_1^0)}{k_B T}\right)$$

$$\underline{X_N = N\left\{X_1 \exp\left(\frac{\boxed{\mu_1^0 - \mu_N^0}}{k_B T}\right)\right\}^N}, \qquad \underline{c = \sum_1^{\infty} X_N}$$

$$X_N(N)$$

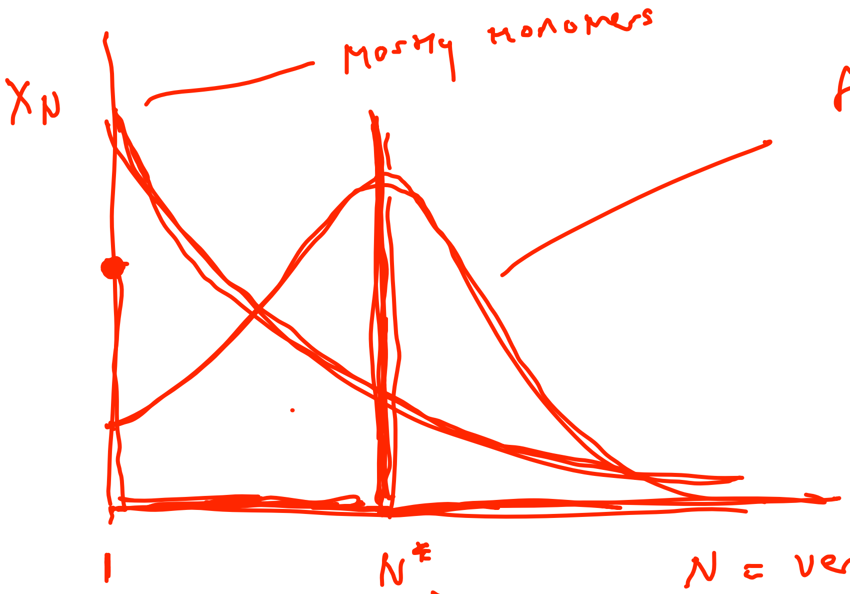

special size ?

favored size

$$\underline{\mu_N^0} < \underline{\mu_1^0}$$

$\underline{\text{if}}$ $\mu_1^0 = \mu_2^0 = \mu_N^0 \longrightarrow X_N = N X_1^N$

N > 1
N >> 1

$X_1 < 1$

$$\underline{X_N \ll 1}$$

Mostly Monomers in solution

in all cases $X_N(N)$ a distribution

simple shapes

(1) rod / chain

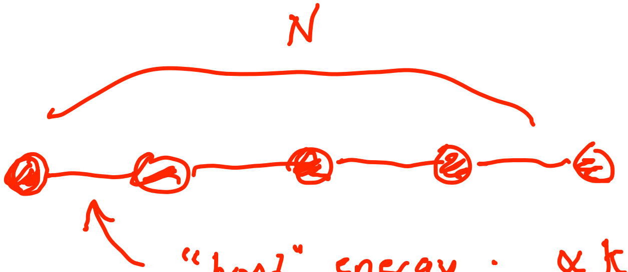

"bond" energy : $\underline{\underline{\alpha k_b T}}$

for a N-length,

$$N \mu_N^0 = -(N-1)\alpha k_b T$$

$$\mu_N^0 = \frac{-(N-1)}{N}\alpha k_b T$$

$$\mu_N^0 = -\alpha k_b T + \frac{\alpha k_b T}{N}$$

Ideal aggregate shapes – bond models

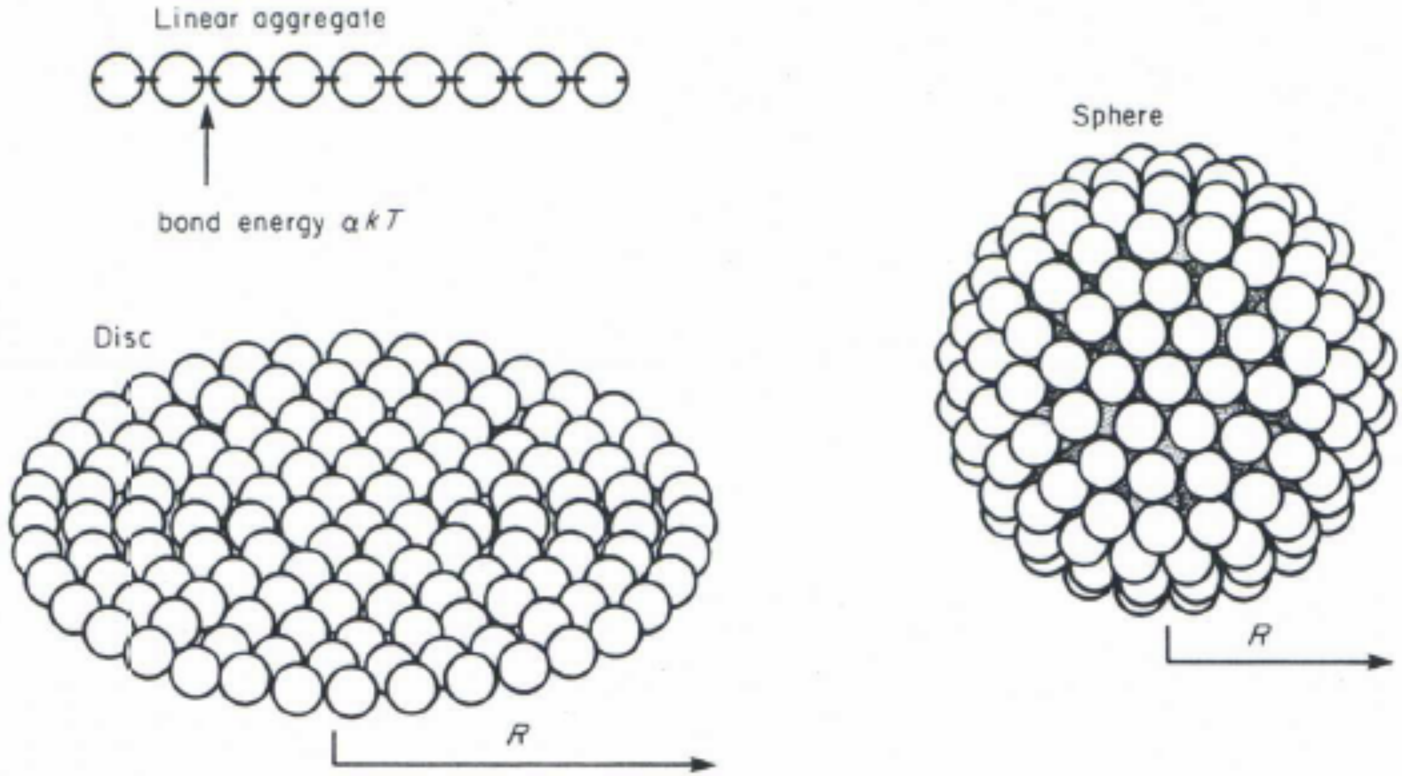

Fig. 16.4. One-, two- and three-dimensional structures formed by the association of identical monomer units in solution.

Israelachvili.

Critical micelle concentration (CMC)

$$\mu_N^0 = \mu_\infty^0 + \frac{\alpha KT}{N^p}$$

α = bonding; p = shape

interactions

$p = 1$

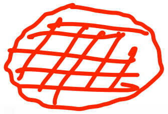

$p = 1/2$

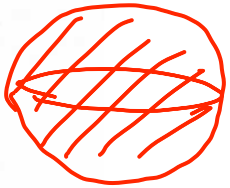

$p = 1/3$

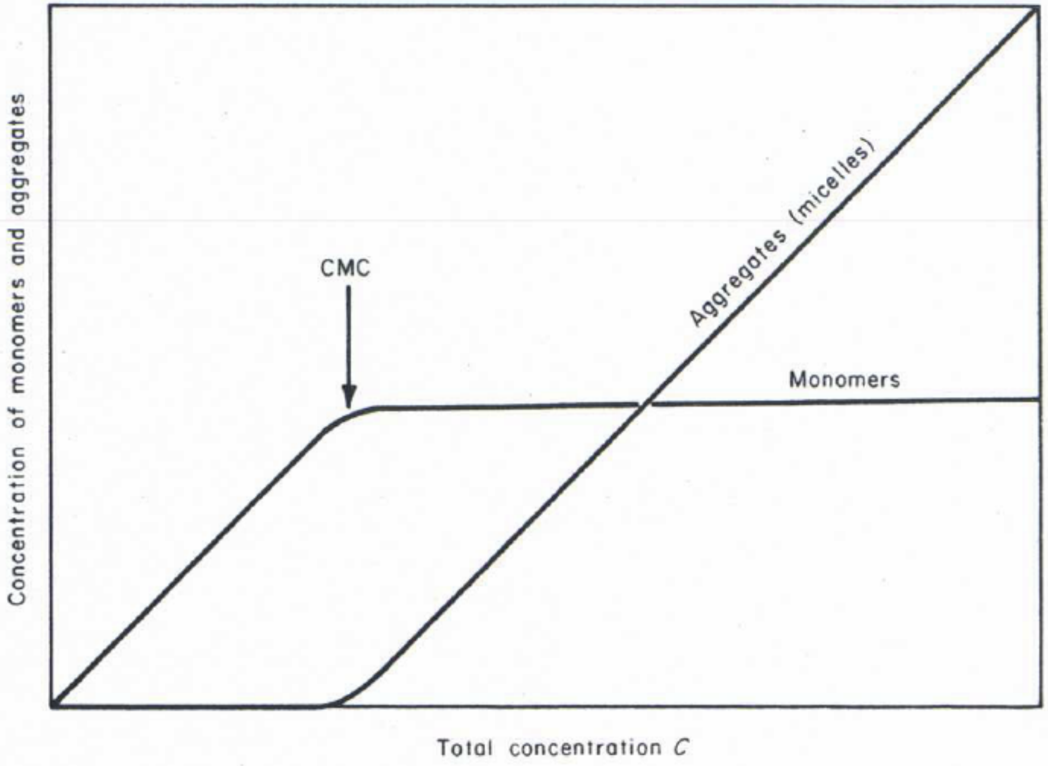

Fig. 16.5. Monomer and aggregate concentrations as a function of total concentration (schematic). Most single-chained surfactants containing 12–16 carbons per chain have their CMC in the range 10^{-2}–10^{-5} M, while the corresponding double-chained surfactants have much lower CMC values due to their greater hydrophobicity. Some important CMC values are listed in Table 16.2.

Israelachvili.

Real cases

- If $\mu_N(N)$ is a smooth decay:
  - bulk aggregation occurs at the CMC
  - there is a distribution of micelles before the CMC, but monomers dominate
- If $\mu_N(N)$ has a local minimum
  - the concentraton of monomers is fixed above the CMC, and new monomers go into aggregates of the stable size
  - there is always a size distribution about the critical size

Size distribution

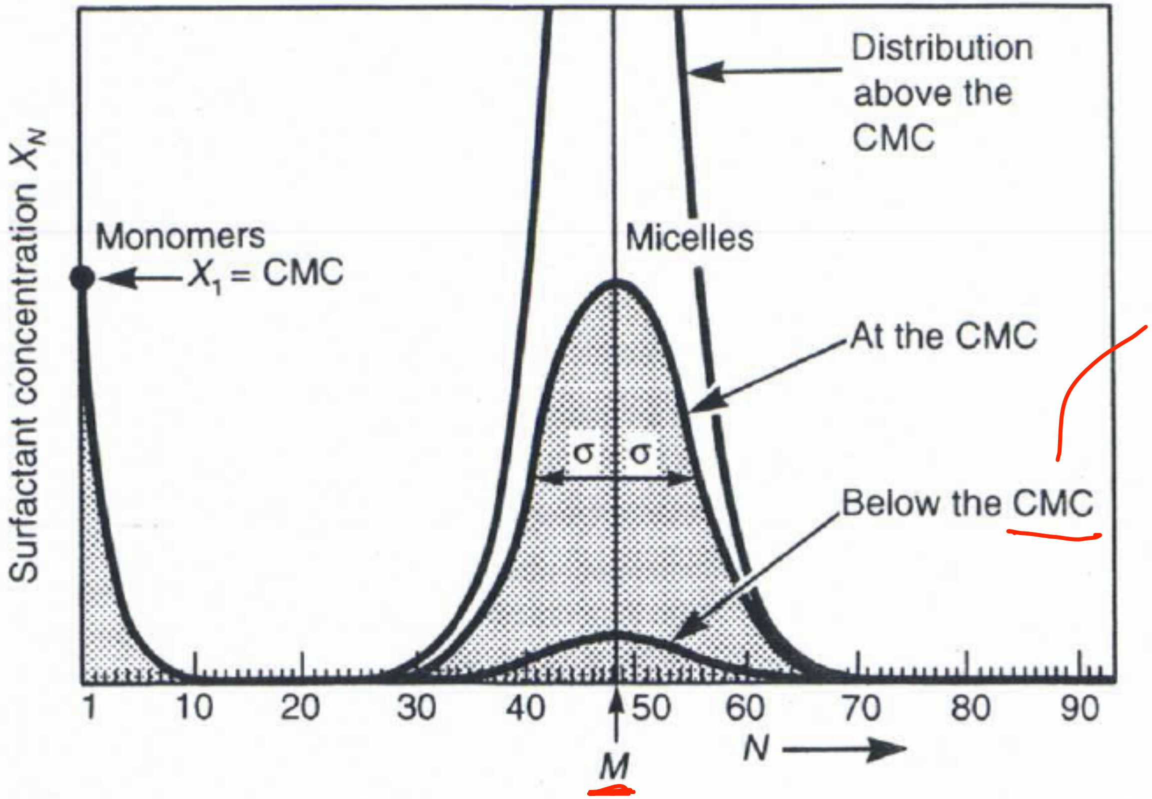

critical concentration

Fig. 16.6. Distribution of molecules X_N as a function of aggregation number N. Near the CMC (shaded region) we have $X_1 \approx X_M$ where the mean micellar aggregation number is M. For spherical micelles, the distribution about M is near Gaussian with standard deviation $\sigma \approx \sqrt{M}$ (see Section 17.4).

Israelachvili.

Normal versus reverse micelles

Normal

Closed “cage”

→ Limits diffusion and size

→ Water droplets in oil

Reverse

Open

→ Limits size

→ Oil droplets in water

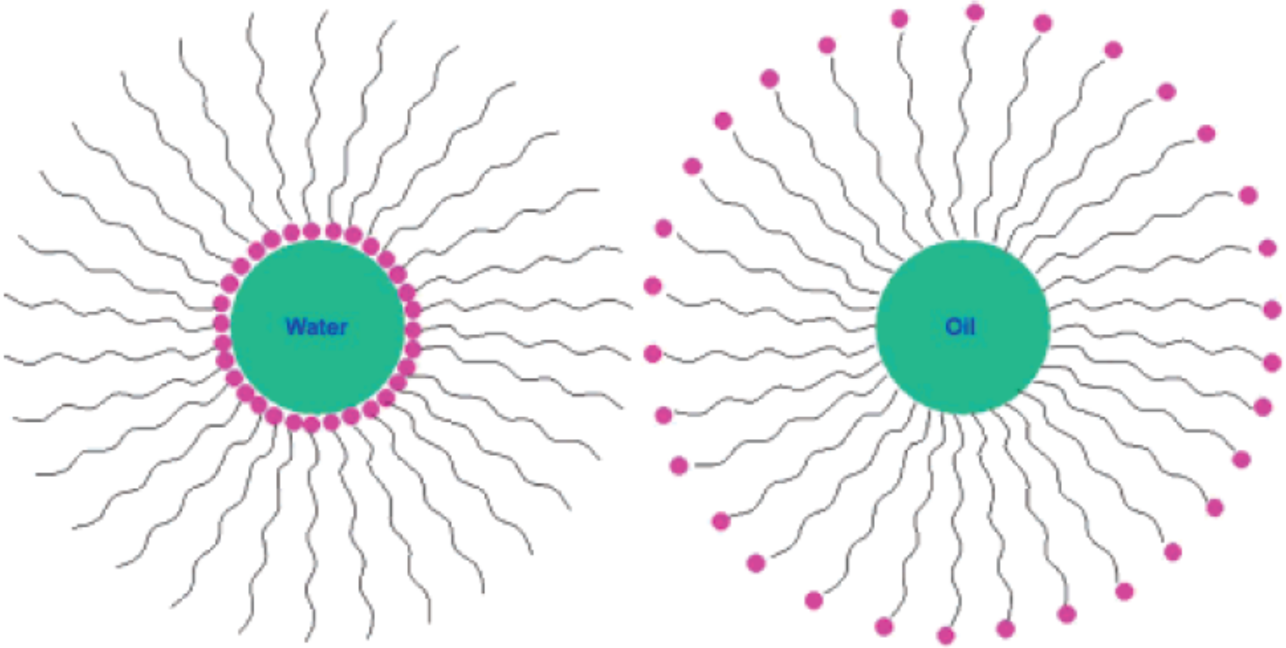

Figure 7. Reverse micelle and normal micelle structures.

Burda.

Exemplary micelle phase diagram

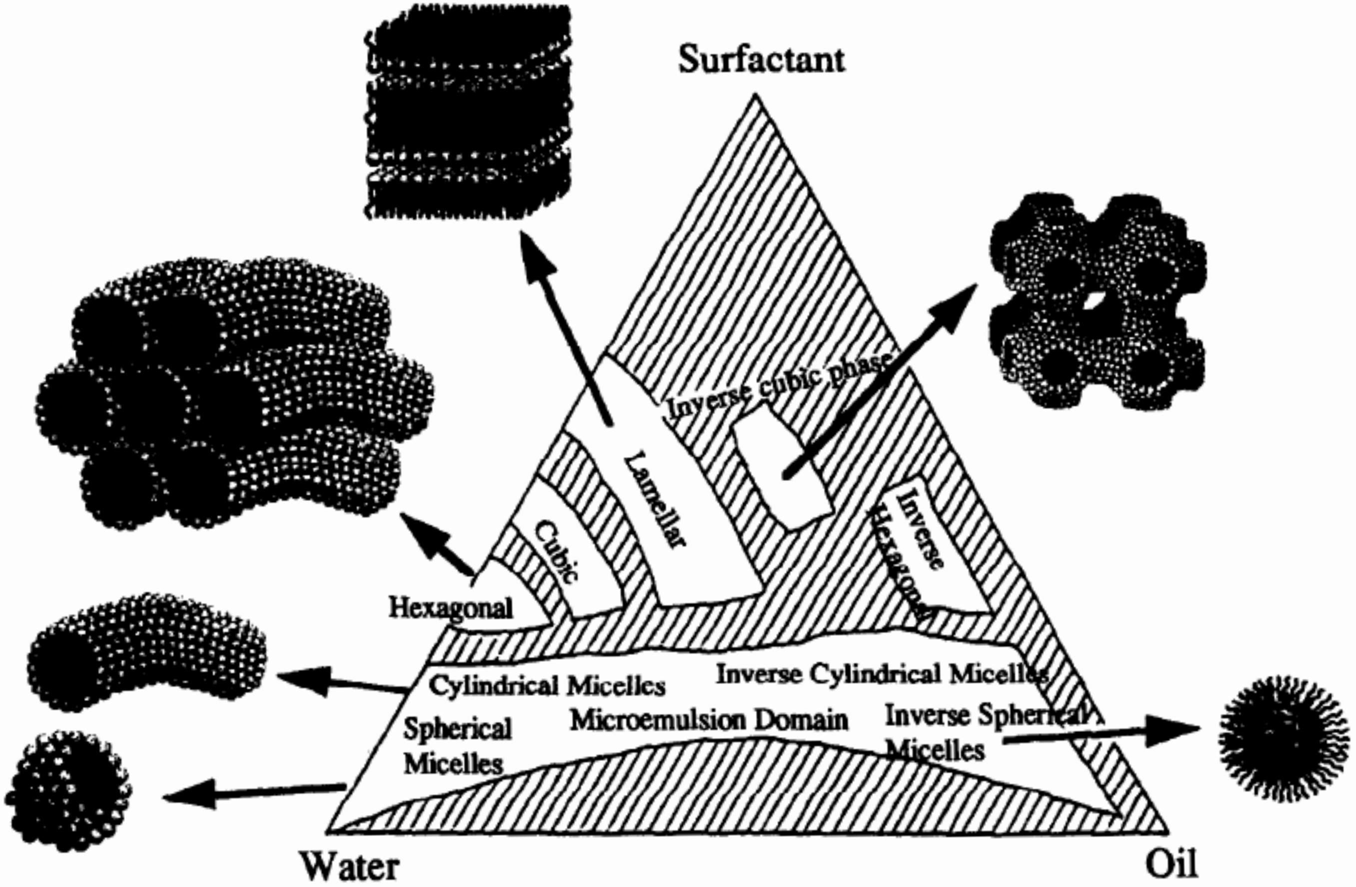

Fig. 9. A schematic phase diagram of surfactant–oil–water systems showing a variety of self-assembled structures that can be used as a *template for materials synthesis* (adapted from Ref. [48a, b, and c]).

J. Liu et al. / Adv. Colloid Interface Sci. 69 (1996) 131–180

151

→ **Many shapes/sizes are possible**

NP synthesis using reverse micelles

Approach I

- Mix two sets of reverse micelles, which were prepared separately
- Mixing causes micelles (A + B) to interact, and exchange of contents causes NP formation

Approach II

- Prepare reverse micelles and mix this solution with a reactant (e.g., a metal salt) that is water-soluble
- Reactant enters the micelle and is stored there

Burda.

Ordered nanoparticle arrays by self-assembly: micellar solutions and block copolymer films

Like a nanoparticle-filled photoresist

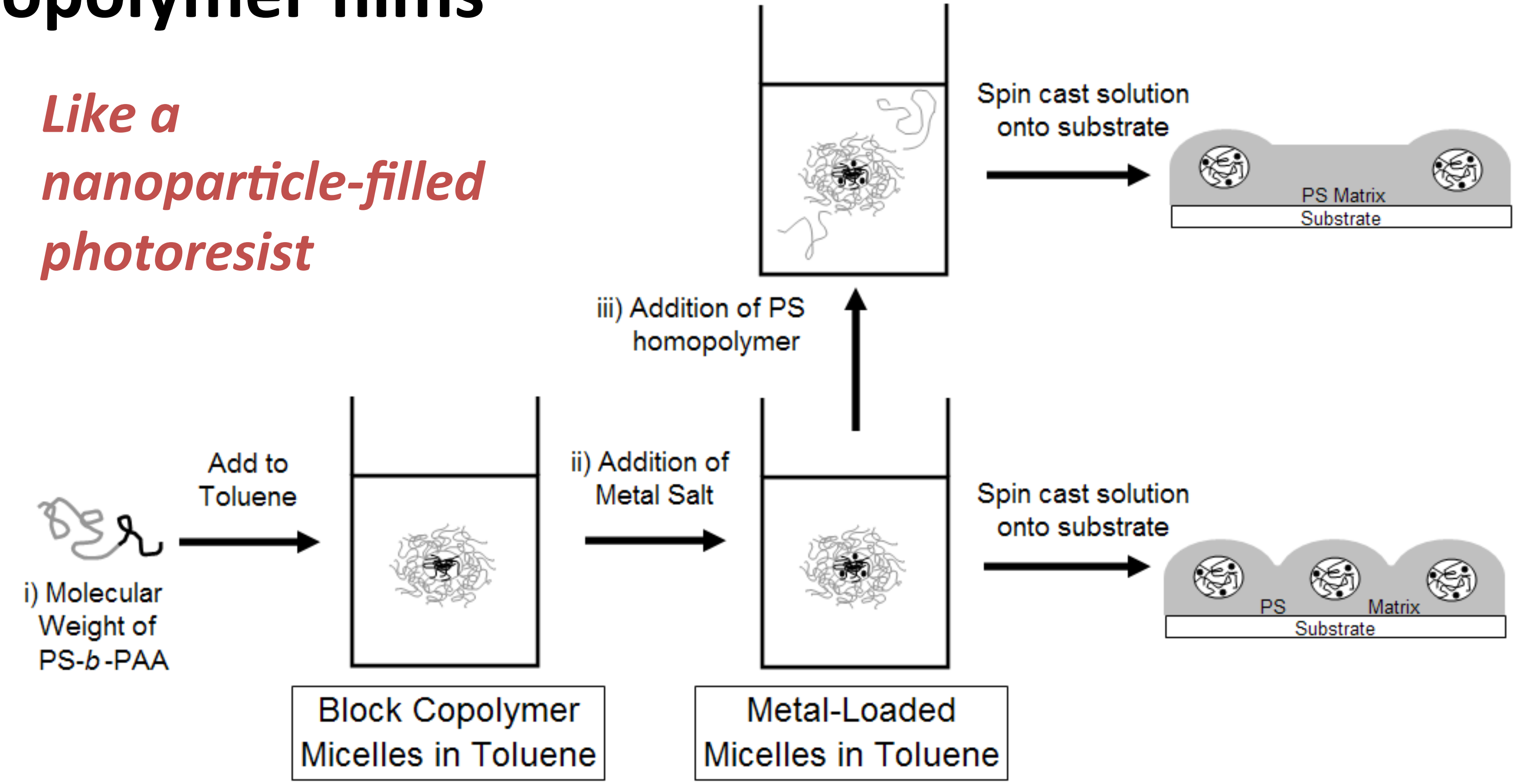

iii) Addition of PS homopolymer

Spin cast solution onto substrate

PS Matrix

Substrate

i) Molecular Weight of PS-*b*-PAA

Add to Toluene

ii) Addition of Metal Salt

Spin cast solution onto substrate

PS

Matrix

Substrate

Block Copolymer Micelles in Toluene

Metal-Loaded Micelles in Toluene

- **Micelle size = nanoparticle size**
- **Homopolymer chain length = particle spacing**

R. Bennett, R. Cohen, et al.

Block copolymers (BCPs)

- Chain of two chemically distinct polymer blocks, which are thermodynamically incompatible, e.g., repel each other
- Chains often must adopt extended configurations (i.e., not bunched) to keep dissimilar portions apart

Diblock

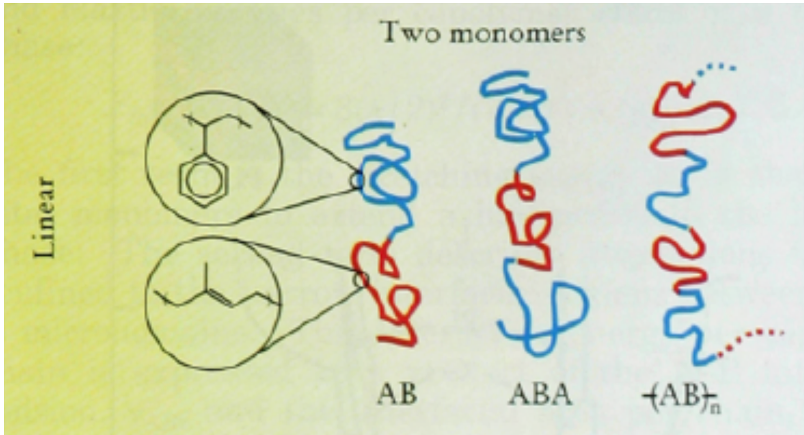

- e.g., PS-b-PMMA = polystyrene-b-poly (methyl methacrylate)
- usually made by first polymerizing styrene, and then subsequently polymerizing MMA from the reactive end of the polystyrene chains

- Blocks give a combination of properties, e.g., low-temperature flexibility and high-temperature resilience
- Used in upholstery foam, adhesive tape, bandages, asphalt,…

Bates and Fredrickson, *Physics Today* February 1999, p. 32-38.

Self-assembly by phase separation

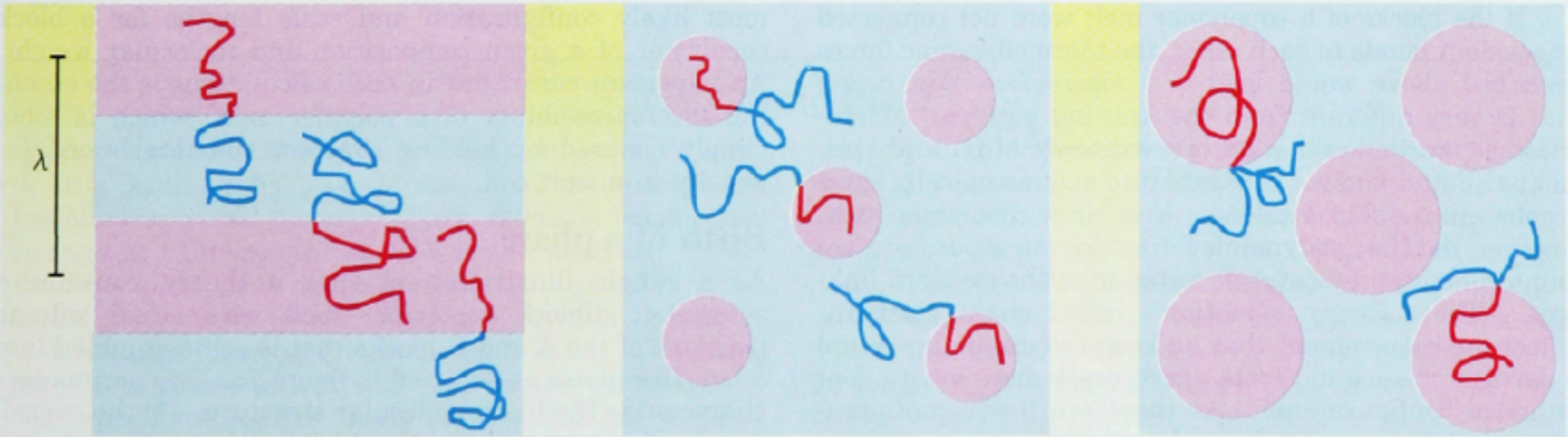

$f_A = 1/2$
AB linear

$f_A > 1/2$
AB linear

$f_A = 1/2$
A_2B branched

FIGURE 2. DIBLOCK MORPHOLOGY depends on block composition. Interfacial curvature of block copolymers can be controlled by adjusting the composition f or changing the molecular architecture. Shaded regions are block-segregated microdomains colored according to monomer type, with blue for type A and red for type B monomers. **a:** Self-assembly of symmetric ($f_A = f_B = 1/2$) linear AB diblocks leads to a lamellar morphology. **b:** Increasing the volume fraction of one block (in this case, $f_A > 1/2$) induces interfacial curvature, resulting in a nonlamellar morphology, such as cylindrical or spherical. **c:** A branched A_2B architecture can result in a nonlamellar morphology even in a compositionally symmetric molecule, due to asymmetric interfacial crowding.

Bates and Fredrickson, *Physics Today* February 1999, p. 32-38.

Self-assembly by phase separation

Theory **Experiment**

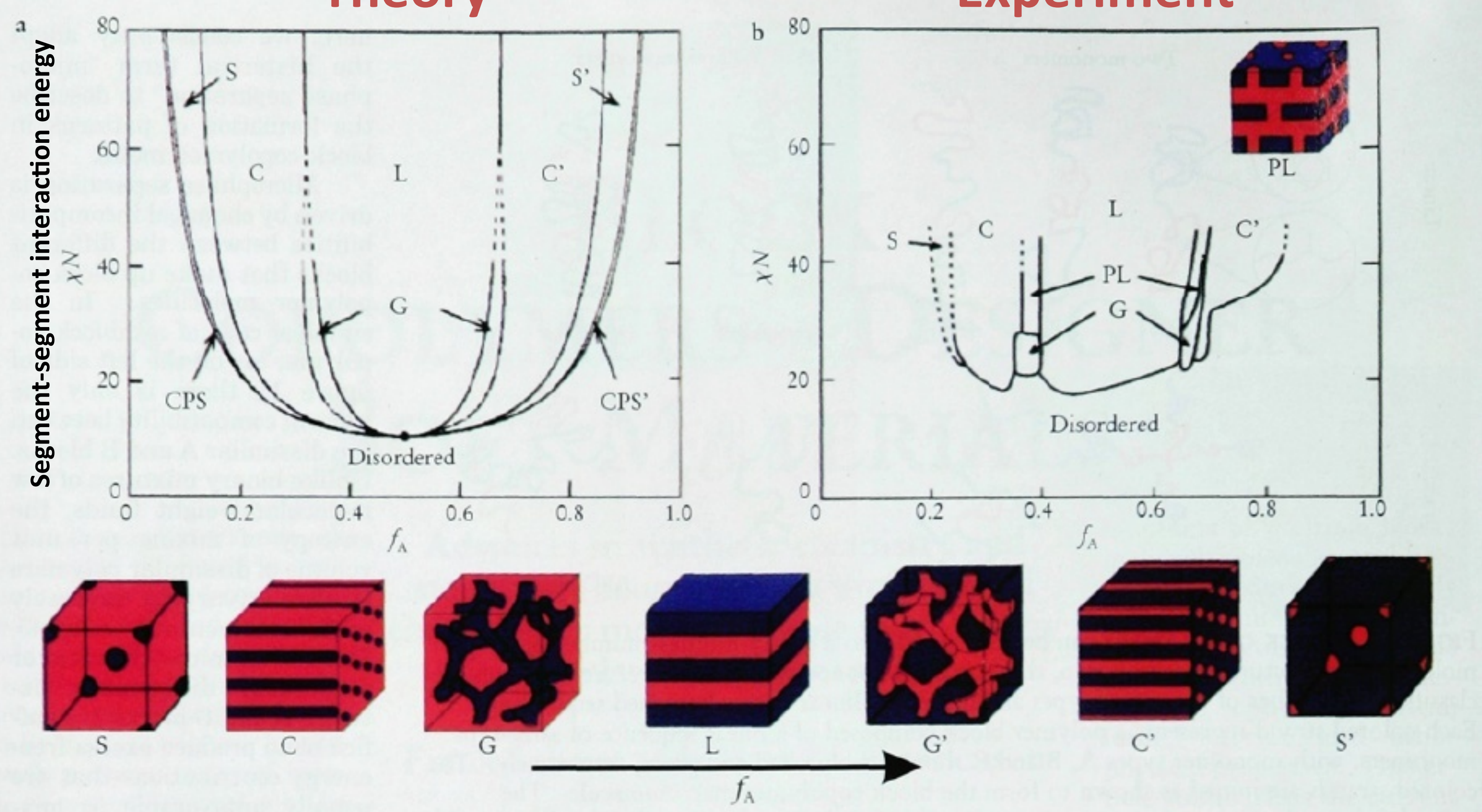

FIGURE 3. PHASE DIAGRAM for linear AB diblock copolymers, comparing theory and experiment. **a:** Self-consistent mean-field theory[8] predicts four equilibrium morphologies: spherical (S), cylindrical (C), gyroid (G) and lamellar (L), depending on the composition f and combination parameter χN. Here, χ is the segment–segment interaction energy (proportional to the heat of mixing A and B segments) and N is the degree of polymerization (number of monomers of all types per macromolecule). **b:** Experimental phase portrait for poly(isoprene-styrene) diblock copolymers.[9] The resemblance to the theoretical diagram is remarkable, though there are important differences, as discussed in the text. One difference is the observed PL phase, which is actually metastable. Shown at the bottom of the figure is a representation of the equilibrium microdomain structures as f_A is increased for fixed χN, with type A and B monomers confined to blue and red regions, respectively.

Bates and Fredrickson, *Physics Today* February 1999, p. 32-38.

BCP designs: blocks, branches

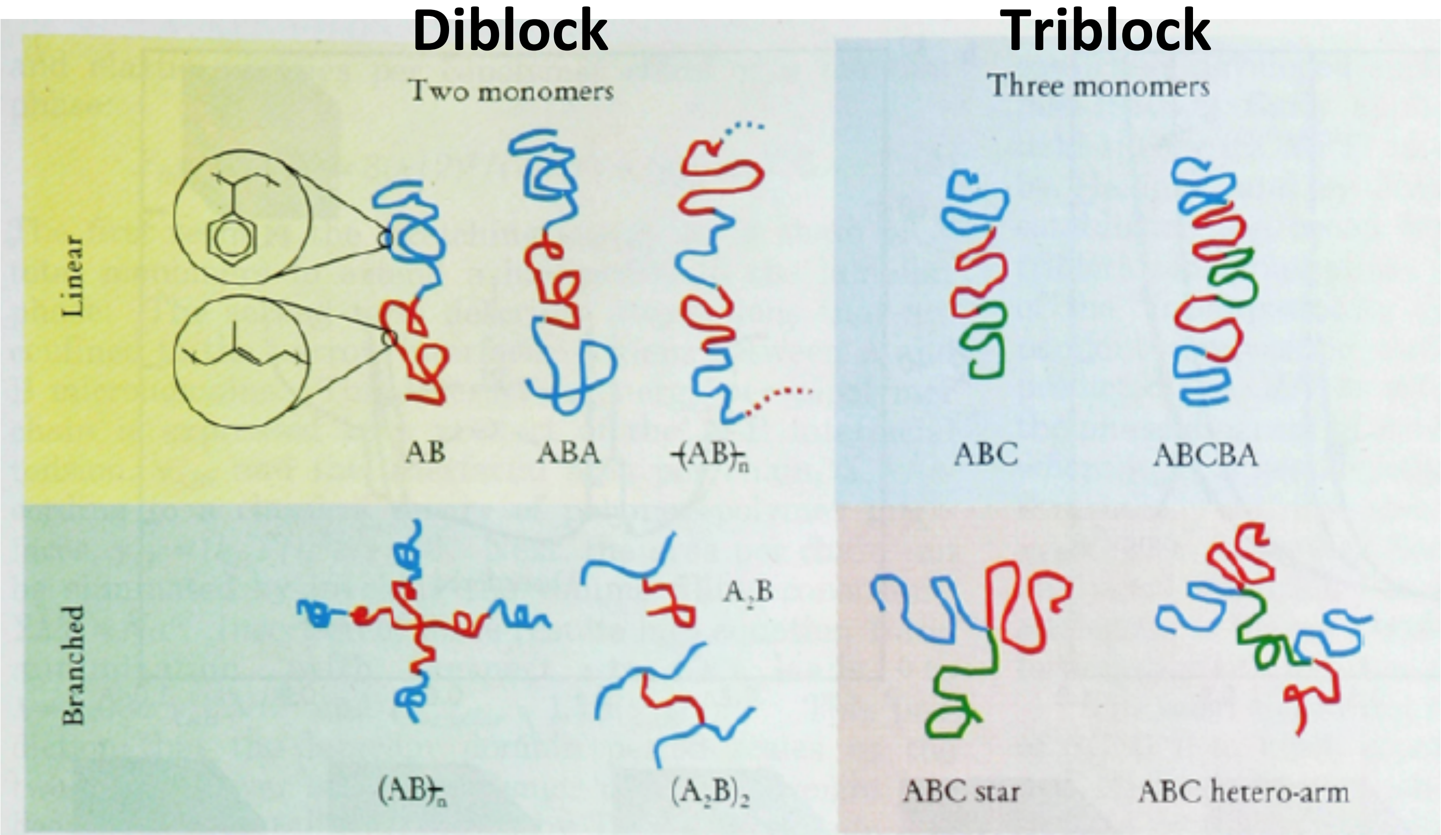

FIGURE 1. BLOCK COPOLYMERS can be configured into a nearly limitless number of molecular architectures based on two, three or more monomer types. Here, architectures are classified by number of monomer types and topology (linear versus branched sequencing). Each colored strand represents a polymer block composed of a linear sequence of same-type monomers, with monomer types A, B and C shown as blue, red and green, respectively. The colored strands are joined as shown to form the block copolymer macromolecule. The upper-left inset shows two representative monomer chemical structures, with the diameter of the circle showing the typical monomer length scale *a*.

Bates and Fredrickson, *Physics Today* February 1999, p. 32-38.

Templated self-assembly of BCPs

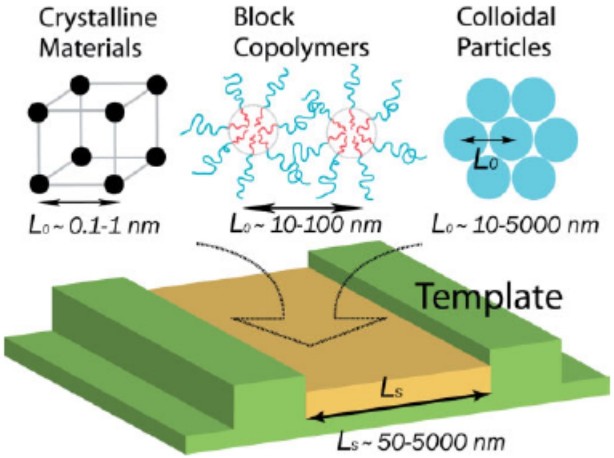

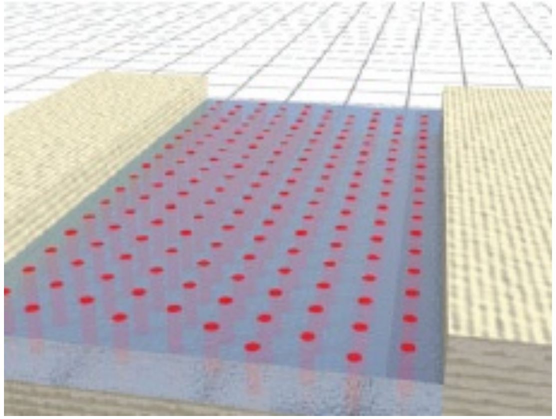

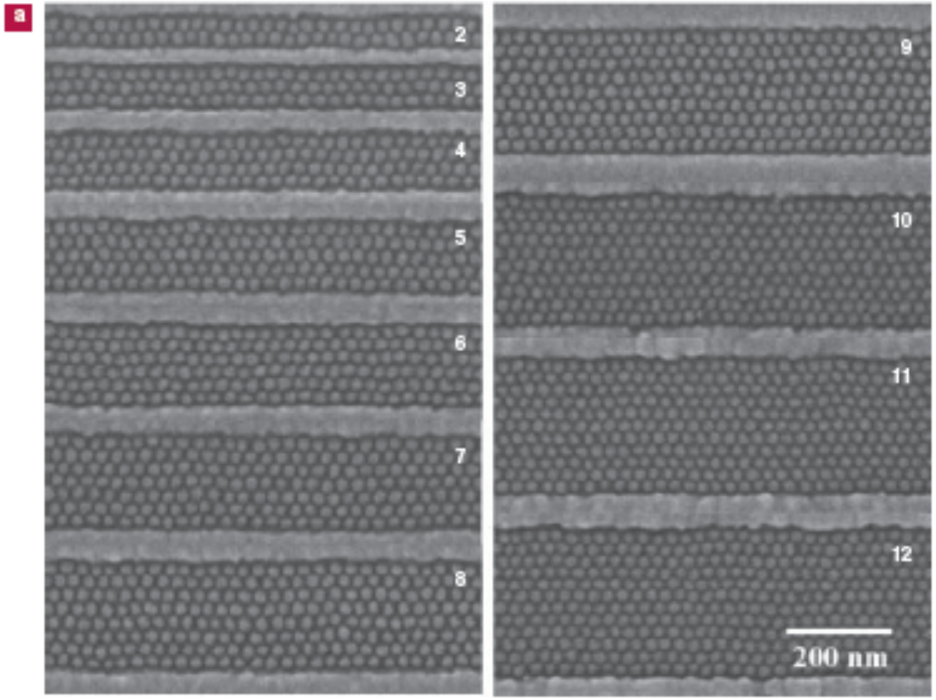

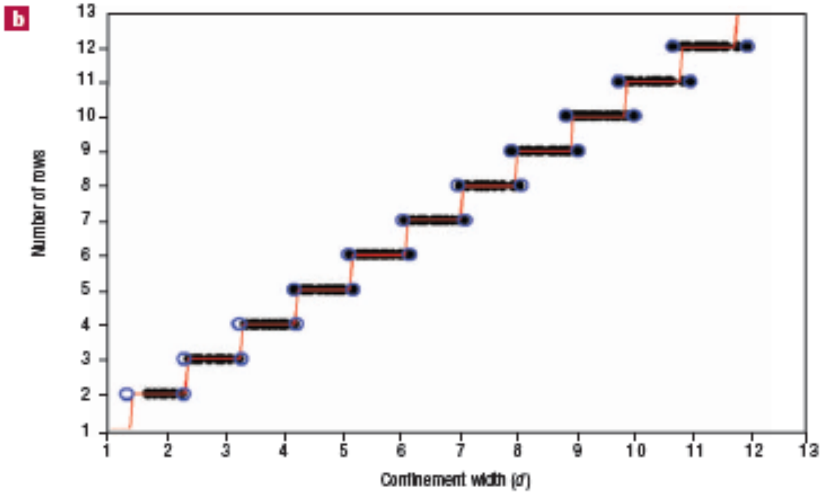

Cheng et al., *Nature Materials* 3:823-828, 2004.

BCP films as etch masks

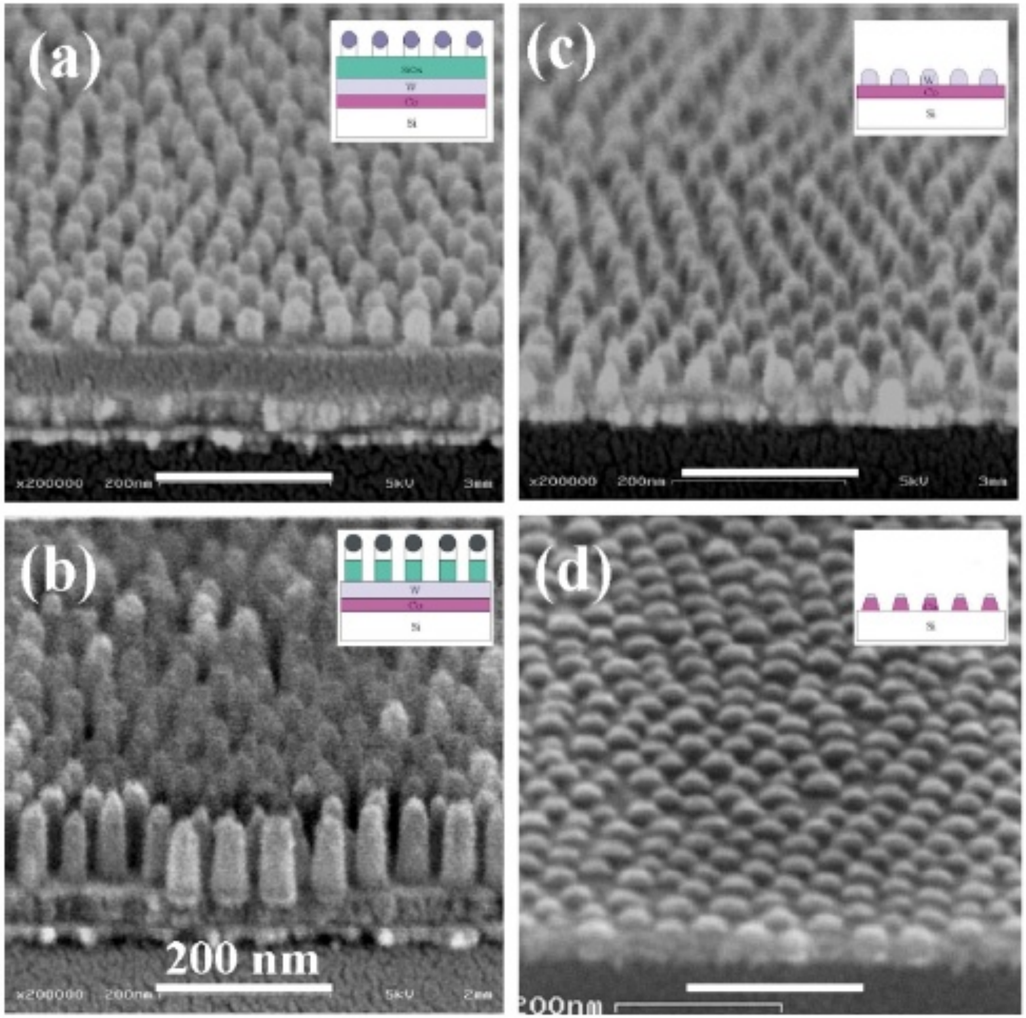

Fig. 7. Tilted SEM micrographs of the fabrication process of Co dot array using PS-PFS BCPs. (a) An O_2-RIE treated block copolymer thin film on a multilayer of silica, the metallic films and the silicon substrate. (b) Pillars of silicon oxide capped with oxidized PFS after CHF3-RIE. (c) W (tungsten) hard mask on top of a Co layer. (d) Co dot array produced Ne ion-beam etching. (Reprinted with permission from *Adv Mater* [91]. WILEY-VCH, STM-Copyright & Licenses (2001)).

Park et al. *Polymer* 44:6725-6760, 2003.

Triblock morphologies

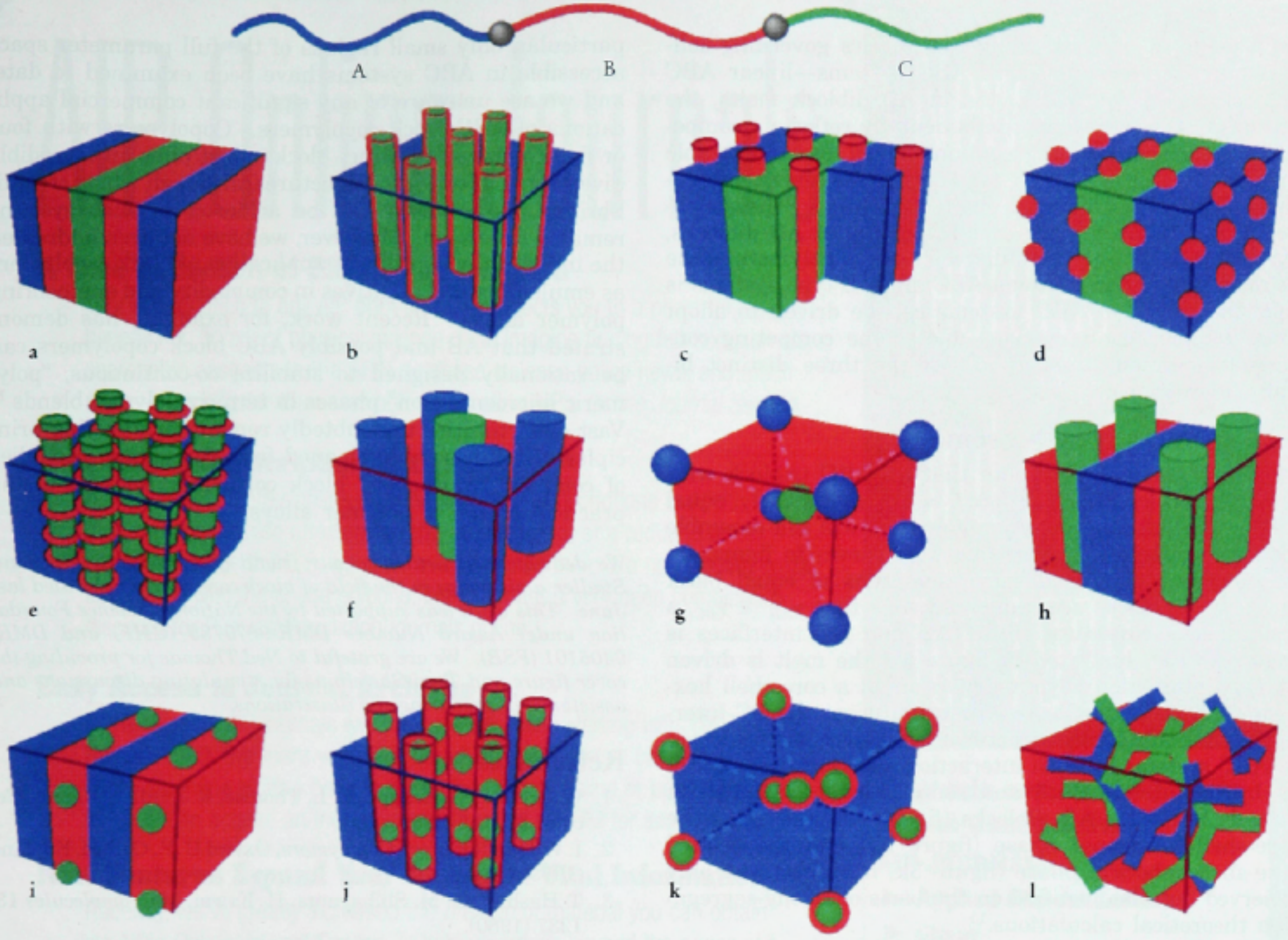

FIGURE 5. MORPHOLOGIES FOR LINEAR ABC triblock copolymers. A combination of block sequence (ABC, ACB, BAC), composition and block molecular weights provides an enormous parameter space for the creation of new morphologies. Microdomains are colored as shown by the copolymer strand at the top, with monomer types A, B and C confined to regions colored blue, red and green, respectively. (Adapted from Zheng and Wang in ref. 13.)

Bates and Fredrickson, *Physics Today* February 1999, p. 32-38.

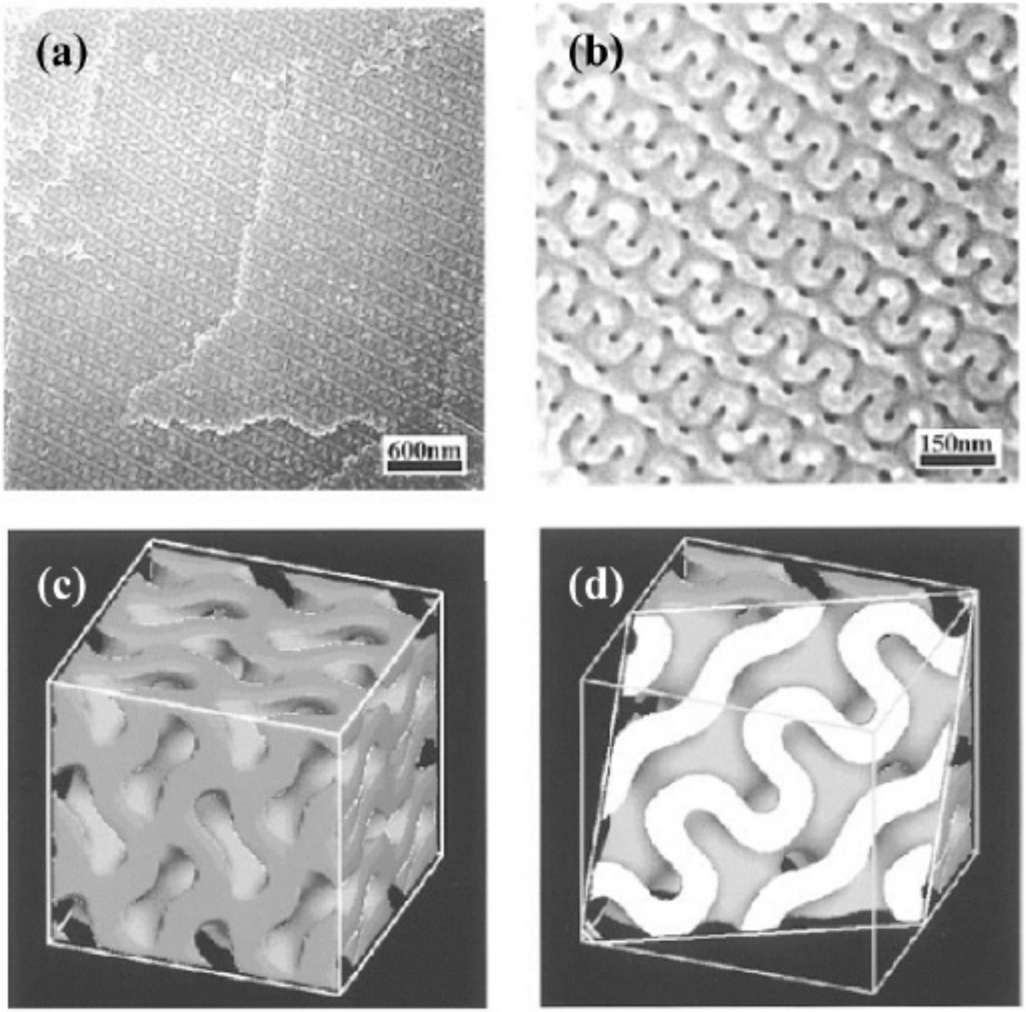

Fig. 2. SEM micrographs showing a bicontinuous nanochannel in the matrix of PS with two different magnifications ((a), (b)) and computer graphics of a double gyroid network: (c) a 3D view and (d) a 2D intersection cut along the (211) direction. (c) shows a solid model in which only the matrix phase, corresponding to the PS matrix in our specimens, is shown. In (d), the bright domain corresponds to the PS matrix and the gray and dark phases correspond to the degraded PI phase. (Reprinted with permission from *Langmuir* [42]. Copyright (1997) American Chemical Society).

Park et al. *Polymer* 44:6725-6760, 2003.

Ordered nanoparticle arrays by self-assembly: micellar solutions and block copolymer films

Like a nanoparticle-filled photoresist

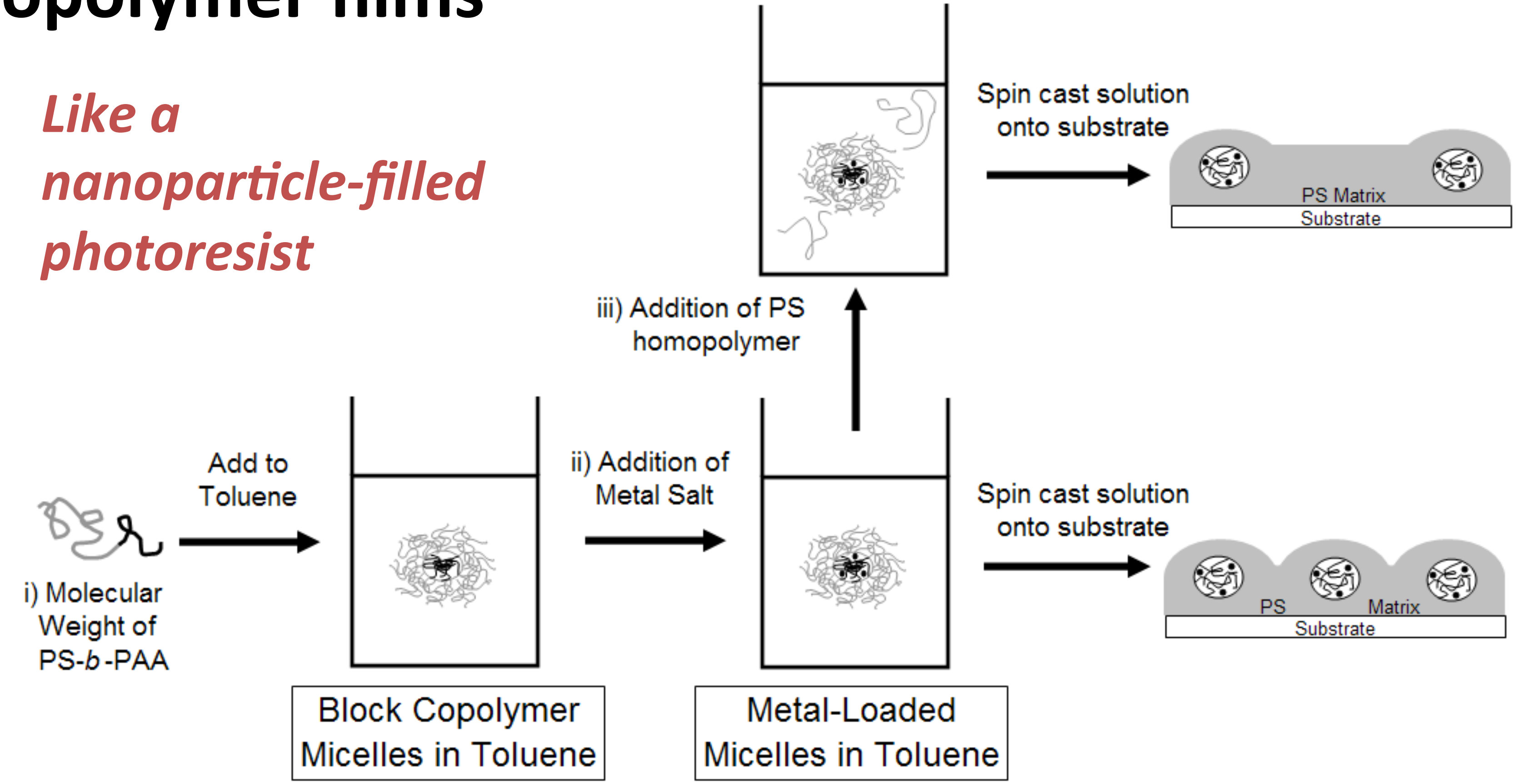

- Micelle size = nanoparticle size
- Homopolymer chain length = particle spacing

R. Bennett, R. Cohen, et al.

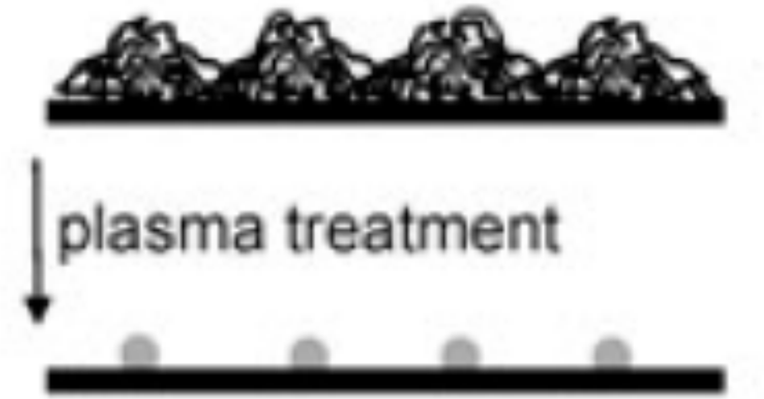

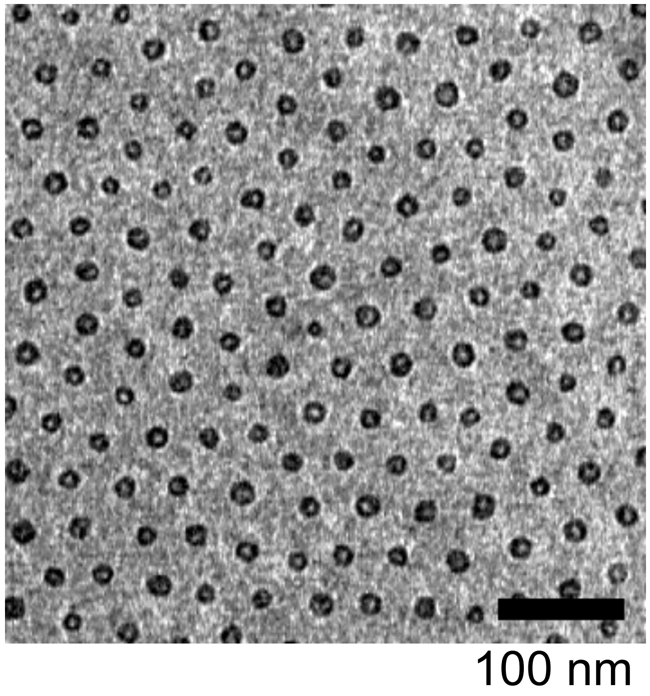

→ *Independent control of size and spacing*

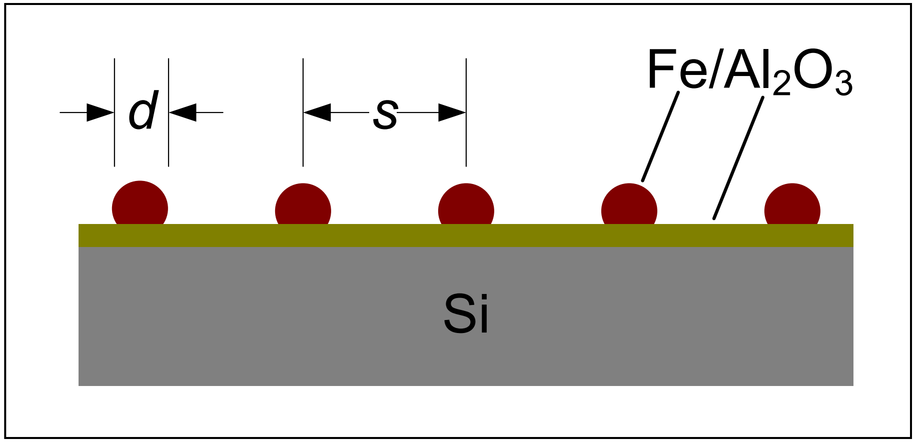

R. Bennett, R. Cohen, et al.

CNT film and forest growth from BCP-templated catalyst films

Q: What is the critical catalyst density for vertically aligned growth?

Before Growth

Particle diameter 16±2 nm

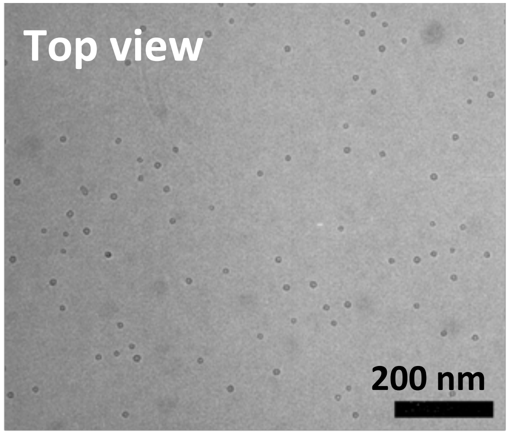

6×10^{9} particles/cm^2

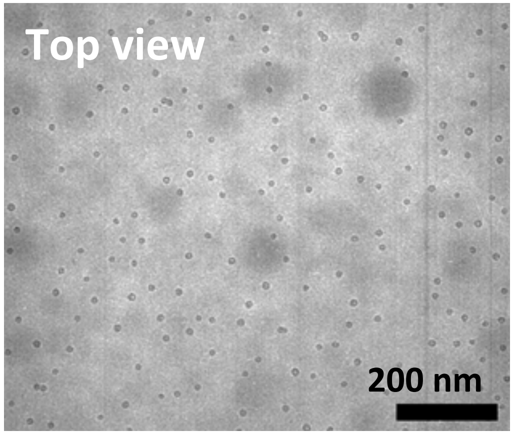

2.5×10^{10} particles/cm^2

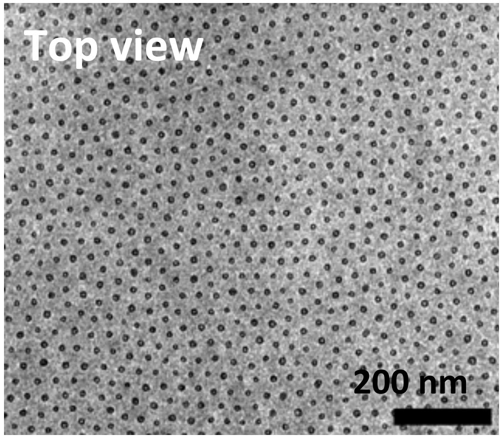

6×10^{10} particles/cm^2

After Growth

CNT diameter 12±2 nm, 8 walls

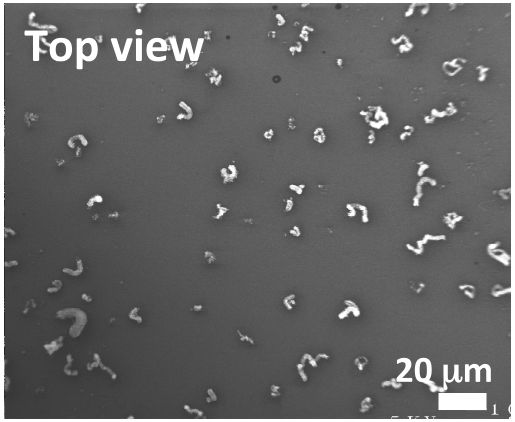

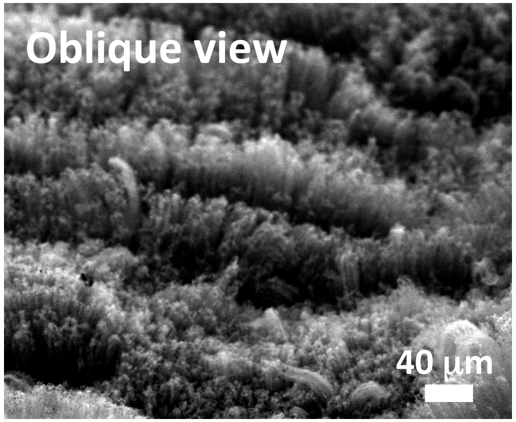

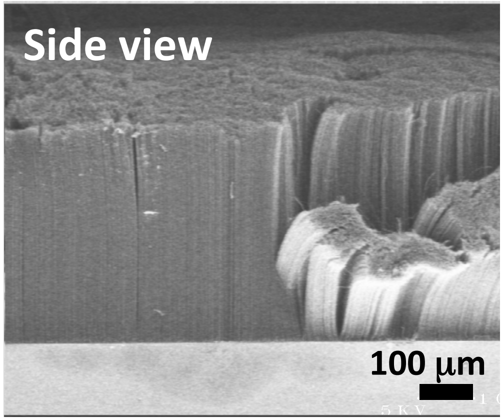

but only ≈5% activity!

Morphology control: Bennett, Hart, Cohen, *Advanced Materials* 18:2274-9, 2006.
Micro-contact printing: Bennett, Hart, et al., *Langmuir* 22:8273-8276, 2006.

BCP films as templates

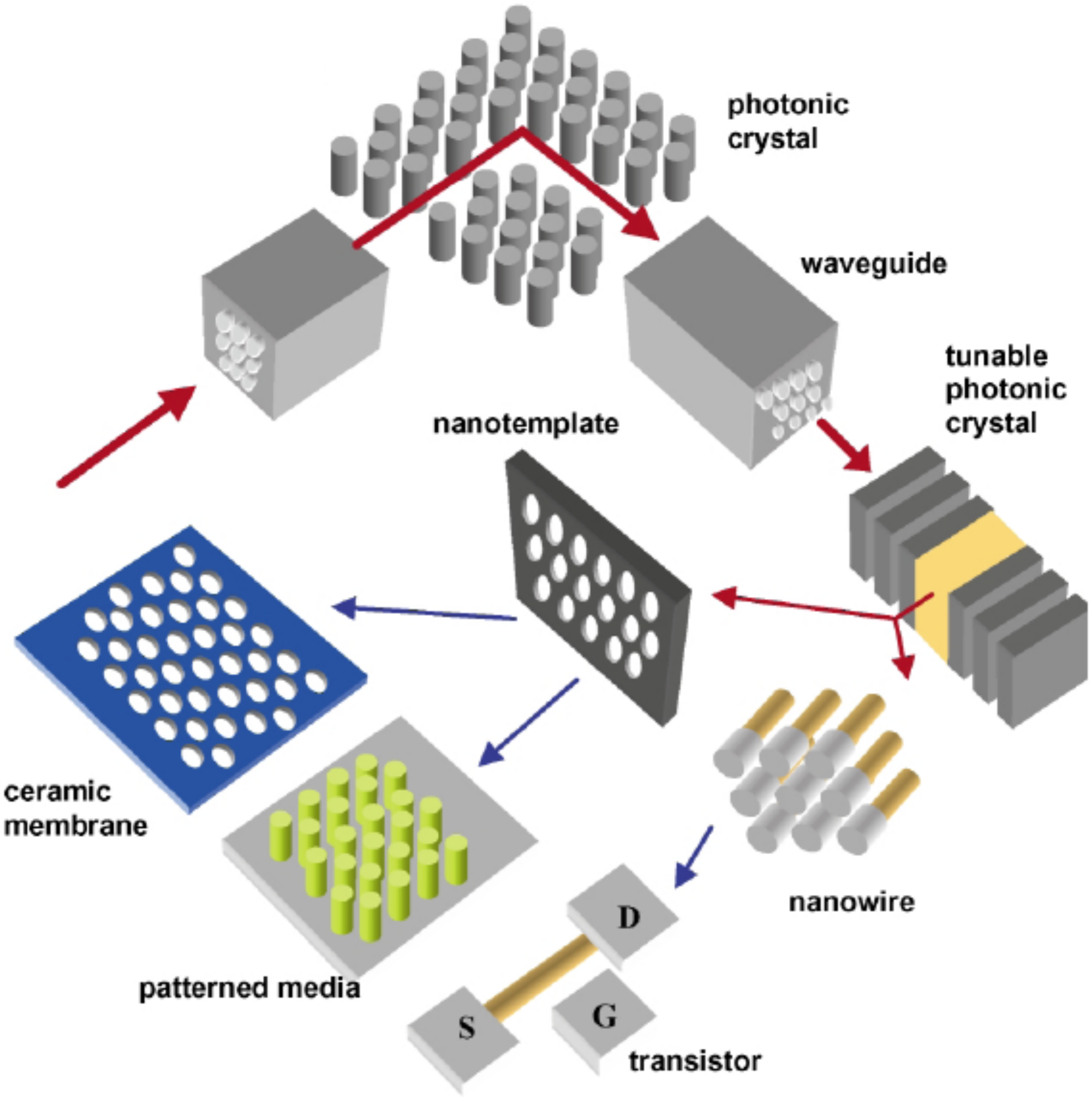

Park et al. *Polymer* 44:6725-6760, 2003.

Assembly of BCPs on SWNTs

- Interplay between BCP phase separation and CNT-induced crystallization of polyethylene (PE)

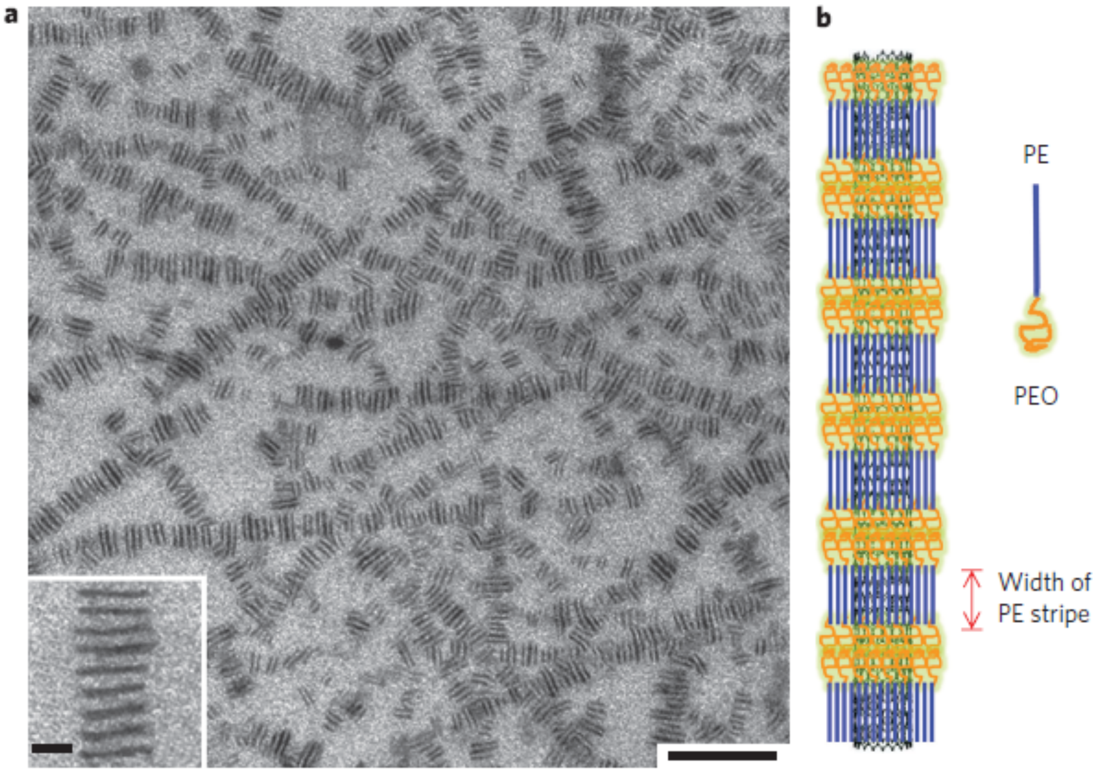

Figure 1 | The alternating pattern of PE-*b*-PEO block copolymers formed on SWNTs. **a**, TEM image of the PE-*b*-PEO decorated SWNTs. The dark and bright stripes are the PEO and PE domains, respectively. The formation of this unique structure is attributed to the subtle interplay between carbon nanotube-induced polymer crystallization and block copolymer phase separation (scale bar, 200 nm). The inset shows an enlarged area (scale bar, 20 nm). **b**, Schematic representation of the arrangement of the PE-*b*-PEO molecules along a SWNT.

Li et al., *Nature Nanotechnology* 4:358-362, 2009.

Mechanism and kinetics

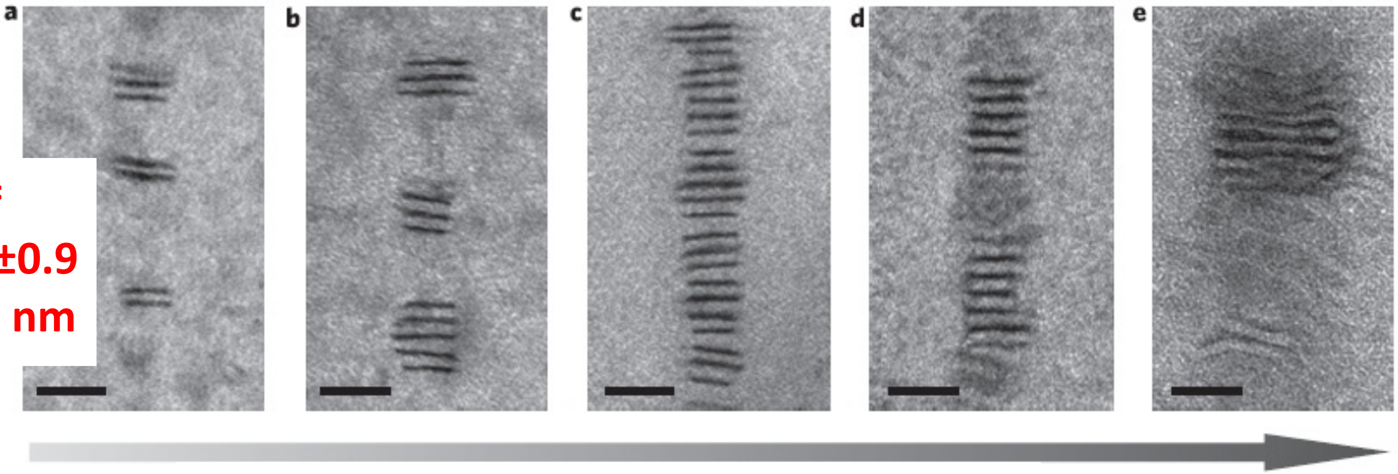

Period = 11.9 ±0.9 nm

Increasing concentration

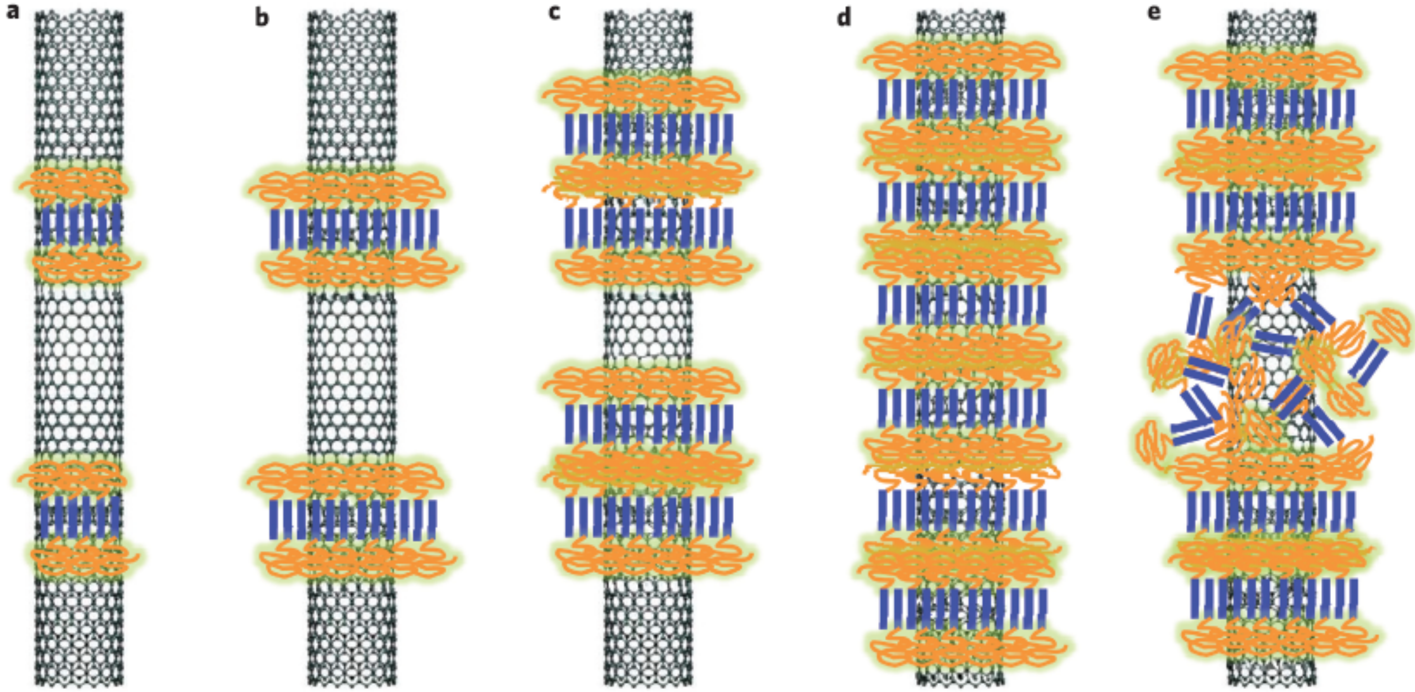

Concentration too high, not enough time for full crystal growth

Li et al., *Nature Nanotechnology* 4:358-362, 2009.

Anchoring Au NPs to BCPs on SWNTs

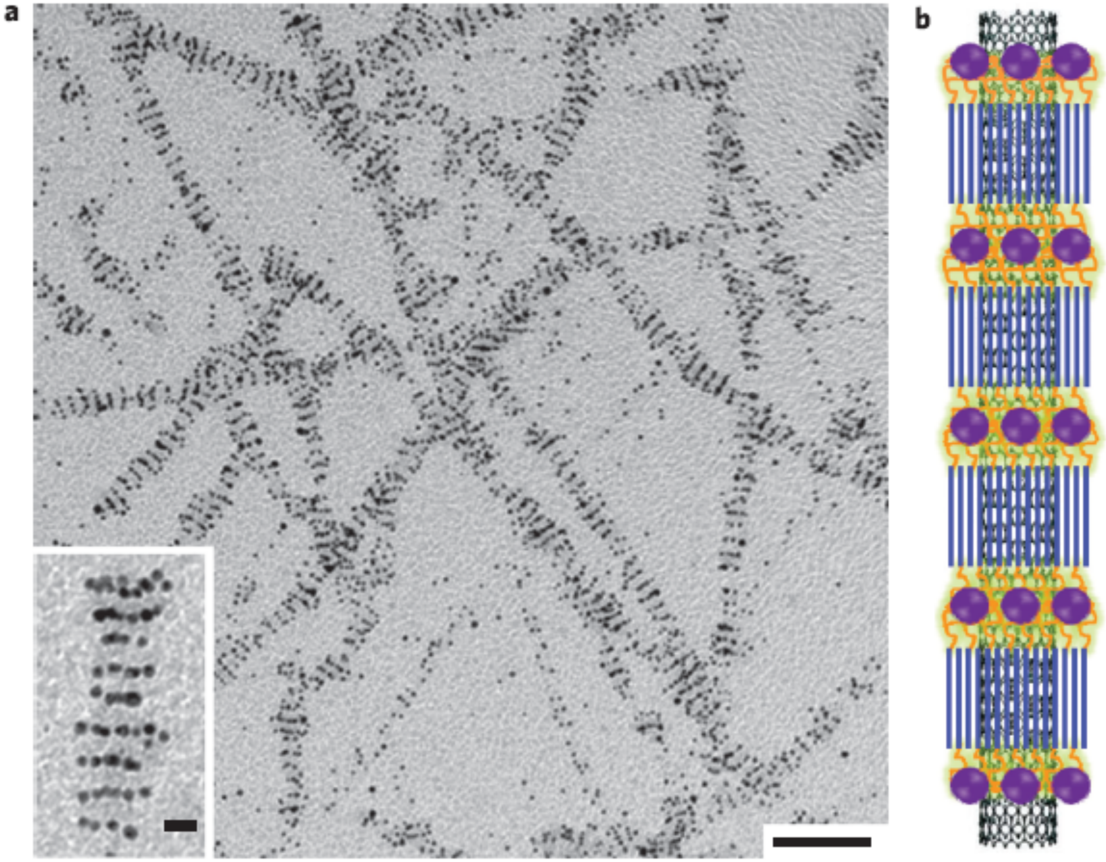

Figure 4 | Periodic immobilization of 5-nm gold nanoparticles on the block copolymer/SWNT hybrid. a, TEM image of the gold nanoparticle-decorated block copolymer/SWNT hybrid. The block copolymer is end-functionalized with a thiol group (scale bar, 100 nm). The inset shows an enlarged area (scale bar, 10 nm). **b**, Schematic representation of the arrangement of the gold nanoparticles and the block copolymer chains along an SWNT.

Li et al., *Nature Nanotechnology* 4:358-362, 2009.